ERS-2 Wind Scatterometer Cyclic Report

From 30th June 2008 to 4th August 2008
Cycle 138

Prepared by:	G. De Chiara	(scat@eo-sppa.org)
Inputs from:	H. Hersbach	(ECMWF)

Table of Content

1 <u>Introduction and Summary</u>

The document includes a summary of the daily quality control made within the DPQC (Data Processing Quality Control) and various sections describing the results of the investigations and studies of "open-problems" related to the Scatterometer. In each section results are shown from the beginning of the mission in order to see the evolution and to outline possible "seasonal" effects. An explanation for the major events which have impacted the performance since launch is given, and comments about the recent events which occurred during the last cycle are included.

This report covers the period 30th June to 4th August 2008 (cycle 138) and includes the results of the monitoring activity performed by ESRIN and ECMWF. This document is available on line at: http://earth.esa.int/pcs/ers/scatt/reports/pcs_cyclic/

Mission events

The following bullets summarize the major mission facts for cycle 138:

• The ERS-2 satellite was piloted in ZGM throughout the cycle.

• The ESACA processor worked nominally without faults.

• The following anomaly occurred on the AMI instrument:

    - AMI in STANDBY/MCMD Refused due to Anomaly 228 ICU REQ 1500 0082 on 26th July from 18.38.30 to 22.40.52.

• On 30th June and 1st July some products delivered with delay due to an Esrin ground segment dissemination facility problem.

• On 17th July meteo files were missing or were delivered with delay to the ground stations due to an Esrin ground segment dissemination problem.

• Missing data from Matera station from 19th July to 31st July due to a ground station hardware problem.

• On 21st July some products delivered with delay due to an Esrin ground segment dissemination facility problem.

• For the entire period of cycle 138, ERS-2 Scatterometer data was used in the 4D-Var data assimilation system at ECMWF.

News on the ERS mission is available on line: http://earth.esa.int/ers/new_ers_news.html

Data Coverage

After the on board tape recorder failure in July 2003, data is acquired in real time whenever

within the visibility range of a ground station. For cycle 138 data coverage has been extended due to the installation of a new ground station in Johannesburg. The data coverage includes: the North-Atlantic, the Mediterranean, the Gulf of Mexico, a small part of the Pacific west from the US, Canada and Central America, a small part of the Atlantic and Indian Ocean around South Africa, the Chinese Sea, a small part of the Indian Ocean South-East of Thailand and Indonesia, and the Southern Ocean close to the Antarctic and south of Australia and New Zealand.

Yaw performance

The result of the monitoring for cycle 138 is an average (per orbit) yaw error angle within the expected nominal range (+/- 2 degrees) for most of the orbit.

Calibration performance

• Calibration data from Transponder are not available since January 2005. This is due to a hardware failure on the transponder. The repair of such device is still under evaluation. The calibration data acquired until 2005 in the ZGM will be re-processed with TOSCA (Tool for Scatterometer Calibration) and the results will be provided in this report when available.

• Due to the regional mission scenario the calibration performances over the Brazilian rain forest are not available because that area is not covered by the ESA ground station. The chance to install a new station to cover the calibration site is still under investigation as well as the possibility to use stable ice area in Greenland or Antarctic to monitor the instrument calibration.

• The Ocean Calibration monitoring is performed by ECMWF. The average backscatter bias level are similarly large, compared to Cycle 137. The gap between the fore/aft and mid beam for the ascending tracks is still considerable. Average bias levels became 0.05 dB more negative (-0.97 dB, was -0.93 dB) being around 0.6 dB more negative than for nominal data in 2000 (around -0.4dB; see Figure 1 of the reports for Cycle 48 to 59). The negative level in bias is not uncommon for this time of the year. The current situation is similar to that of one year ago (see report for Cycle 127). Long-term variations correlate with the yearly cycle, which, given the non-global coverage, is understandable. Therefore, the method of ocean calibration will probably only provide accurate information on calibration levels for globally or yearly data sets.

Instrument performance

• During the cycle 138 the mean transmitted power evolution had a mean decrease of 0.11 dB. This value is similar to the nominal decreasing trend of 0.1 dB/Cycle detected since the beginning of the mission. This parameter will be further monitored in the next cycles.

• The evolution of the noise power during the cycle 138 was stable. The daily average for the Fore and Aft beam noise is around 1.7 ADC (I) and around 1.6 ADC (Q) respectively. For the Mid beam the daily average noise is around 0 ADC.

• During the cycle 138 the Doppler compensation evolution was stable. The daily average of the CoG of the compensated received signal is around 30 Hz and -80 Hz for the Fore and Aft antenna respectively. For the Mid antenna it was around 240 Hz. The standard deviation of the CoG was around 1500 Hz for the Fore and Aft antenna and around 2750 Hz for the Mid antenna.

Timeliness performance

Timeliness performances stayed stable during the cycle 138 for most of the stations. Kiruna and Matera data are delivered in 30 min; for the other stations the delivery delay is ranging between 40 and 50 minutes. In the reporting period a decrease has been detected for Matera stations that reached an average timeliness value of about 25 minutes.

Product performance

During Cycle 138 data was received between 21:15 UTC 30 June 2008 and 20:27 UTC 4 August 2008. Data was grouped into 6-hourly batches (centred around 00, 06, 12 and 18 UTC). Data was received for all batches.

Compared to Cycle 137, the UWI wind speed relative to ECMWF first-guess (FG) fields showed a lower standard deviation (1.29 m/s, was 1.31 m/s). Bias levels were similar as well (on average -1.11 m/s, was -1.10 m/s).

The PCS geophysical monitoring reports a wind speed bias (UWI vs 18 or 24 hour forecast) of 0.9 m/s and a speed bias standard deviation around 1.6 m/s.

The reduced number of nodes available on 30th June is due to a problem in the Esrin

dissemination facility.

The wind direction deviation for cycle 138 was good with more than 98% of the nodes wind direction in agreement with the ECMWF forecast.

2   Calibration Performances

The calibration performances are estimated using three types of target: a man made target (the transponder) and two natural targets (the rain forest and the ocean). This approach allow us to design the correct calibration using a punctual but accurate information from transponders and an extended but noisy information from rain forest and ocean for which the main component of the variance comes from the geophysical evolution of the natural target and from the backscattering models used. These aspects are in the calibration performance monitoring philosophy. The major goals of the calibration monitoring activities are the achievement of a "flat" antenna pattern profile and the assurance of a stable absolute calibration level.

2.1   Gain Constant over transponder

One gain constant is computed per transponder per beam from the actual and simulated two-dimensional echo power, which is given as a function of the orbit time and range time. This parameter clearly indicates the difference between "real instrument" and the mathematic model. In order to acquire data over the transponder the Scatterometer must be set in an appropriate operational mode defined as "Calibration Mode". Since January 2001 with the operations in Zero Gyro Mode (ZGM) the satellite attitude is not stable as it was in the nominal Yaw Steering Mode (YSM). In particular there is a non-predictable variation of the yaw error angle along the orbit. For that reason the gain constant data computed by the CALPROC processor, that assumes a stable orbit, are meaningless and a new calibration processor is under development. In the mean time, data from the Transponder are still acquired and archived for future re-processing. The reprocessed gain constants will be provided in this section when available. For the gain constant computed during the nominal YSM please refer to the Scatterometer cyclic report cycle 60.

2.2   Ocean Calibration

The average sigma0 bias levels (compared to simulated sigma0's based on ECMWF model FG winds) stratified with respect to antenna beam, ascending or descending track and as function of incidence angle (i.e. across-node number) is displayed in Figure 1.

Inter-node and inter-beam dependencies between the fore and aft antenna are similarly large, compared to Cycle 137. The gap between the fore/aft and mid beam for the ascending tracks is considerable. Average bias level became 0.05 dB more negative (-0.97 dB, was -0.93 dB), being around 0.6 dB more negative than for nominal data in 2000 (around -0.4 dB; see Figure 1 of the reports for Cycle 48 to 59). The negative level in bias is not uncommon for the time of this year. The current situation is similar to that of one year ago (see e.g. the report for Cycle 128).

The data volume of descending tracks was about 2% lower than for ascending tracks.
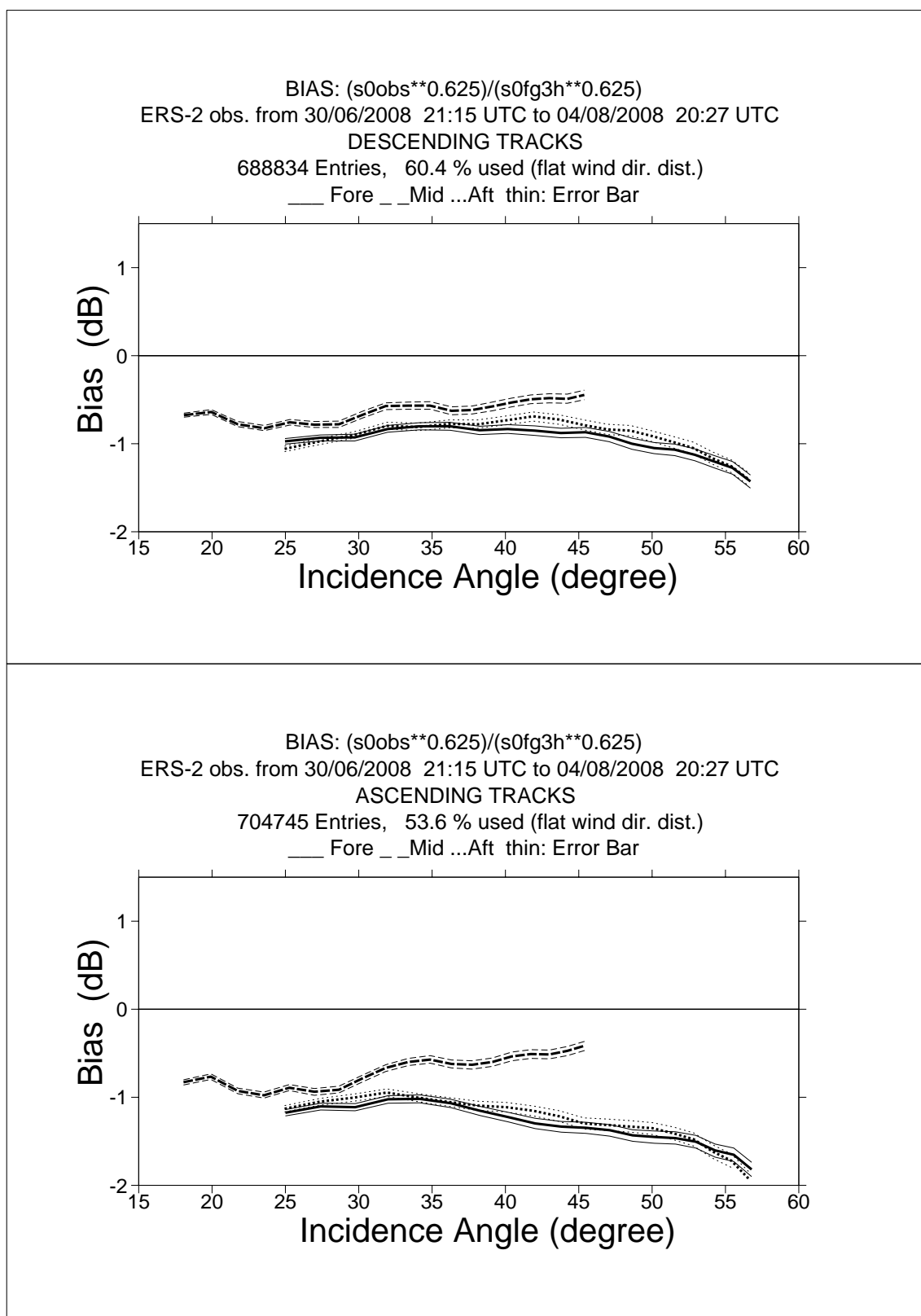
BIAS: (s0obs**0.625)/(s0fg3h**0.625)
ERS-2 obs. from 30/06/2008 21:15 UTC to 04/08/2008 20:27 UTC
DESCENDING TRACKS
688834 Entries,   60.4 % used (flat wind dir. dist.)
___ Fore _ _Mid ...Aft thin: Error Bar

BIAS: (s0obs**0.625)/(s0fg3h**0.625)
ERS-2 obs. from 30/06/2008 21:15 UTC to 04/08/2008 20:27 UTC
ASCENDING TRACKS
704745 Entries,   53.6 % used (flat wind dir. dist.)
___ Fore _ _Mid ...Aft thin: Error Bar

FIGURE 1 ERS-2 Scatterometer Ocean Calibration cycle 138. Ratio of <sigma_0^0.625>/<CMOD4(First Guess)^0.625> converted in dB for the fore beam (solid line), mid beam (dashed line) an aft beam (dotted line), as a function of incidence angle for descending and ascending tracks. The thin lines indicate the error bars on the estimated mean. First-guess winds are based on the in time closest (+3h, +6h, +9h, or +12h) T511 forecast field, and are bilinearly interpolated in space.

2.3   Gamma-nought over the Brazilian rain forest

Although the transponders give accurate measurements of the antenna attenuation at particular points of the antenna pattern, they are not adequate for fine tuning across all incidence angles, as there are simply not enough samples. The tropical rain forest in South America has been used as a reference distributed target. The target at the working frequency (C-band) of ERS-2 Scatterometer acts as a very rough surface, and the transmitted signal is equally scattered in all directions (the target is assumed to follow the isotropic approximation). Consequently, for the angle of incidence used by ERS-2 Scatterometer, the normalized backscattering coefficient (sigma nought) will depend solely on the surface effectively seen by the instrument:

$$S^0 = S \bullet \cos\theta$$

With this hypothesis it is possible to define the following formula:

$$\gamma^0 = \frac{\sigma^0}{\cos\theta}$$

Using the above equation, the gamma nought backscattering coefficient over the rain forest is independent of the incident angle, allowing the measurements from each of the three beams to be compared. The test area used by the PCS is located between 2.5 degrees North and 5.0 degrees south in latitude and 60.5 degrees West and 70.0 degrees West in longitude. That area is actually not covered by the Regional mission scenario (since cycle 86 onwards) and therefore the calibration monitoring activity over the Brazilian rain forest is suspended because no data are available. The chance to continue the monitoring activity with a new receiving station covering the Brazilian rain forest is under investigation. The following paragraphs will report on the results when data will be available.

2.4   Antenna pattern: Gamma-nought as a function of elevation angle

Due to the regional mission scenario data over the Brazilian rain forest are not available. For that reason the antenna patterns in function of the elevation angle have not been computed.

2.5   Antenna pattern: Gamma-nought as a function of incidence angle

Due to the regional mission scenario data over the Brazilian rain forest are not available. For that reason the antenna patterns in function of the incidence angle have not been computed.

2.6   Gamma nought histograms and peak position evolution

As the gamma nought is independent from the incidence angle, the histogram of gamma

nought over the rain forest is characterized by a sharp peak. The time-series of the peak position gives some information on the stability of the calibration. This parameter is computed by fitting the histogram with a normal distribution added to a second order polynomial:

$$F(x) = A_0 \cdot \exp\left(-\frac{z^2}{2}\right) + A_3 + A_4 \cdot x + A_5 \cdot x^2$$

where: $\quad z = \dfrac{x - A_1}{A_2}$

The parameters are computed using a non linear least square method called "gradient expansion". The position of the peak is given by the maximum of the function F(x). The histograms are computed weekly (from Monday to Sunday) for each antenna individually "Fore", "Mid" and "Aft" and for ascending and descending passes with a bin size of 0.02 dB. Due to the regional mission scenario data over the Brazilian rain forest are not available and the histograms have not been computed. For the time series since the beginning of the mission please refer to the Scatterometer cyclic report cycle 86.

2.7   Gamma nought image of the reference area

Due to the regional mission scenario data over the Brazilian rain forest are not available and the histograms have not been computed.

2.8   Sigma nought evolution

Due to the regional mission scenario data over the Brazilian rain forest are not available. For that reason none update has been done to the sigma nought evolution time series. For the time series since the beginning of the mission until June 2003 please refer to the Scatterometer cyclic report cycle 86.

2.9   Antenna temperature evolution over the Rain Forest

Due to the regional mission scenario data over the Brazilian rain forest are not available.
For the time series since the beginning of the mission please refer to the Scatterometer cyclic report cycle 86.

3   Instrument performance

The instrument status is checked by monitoring the following parameters:

• Centre of Gravity (CoG) and standard deviation of the received signal spectrum after the on-ground Doppler Compensation filter. This parameter is useful for the monitoring of the orbit stability, the performances of the Doppler compensation filter, the behavior of the yaw steering mode and the performances of the devices in charge for the satellite attitude (e.g. gyroscopes, Earth sensor, Sun sensor).

• Noise power I and Q channel.

• Internal calibration pulse power.

The latter is an important parameter to monitor the transmitter and receiver chain, the evolution of pulse generator, the High Power Amplifier (HPA), the Traveling Wave Tube (TWT) and the receiver. These parameters are extracted daily from the UWI products and averaged. The evolution of each parameter is characterized by a least square line fit. The coefficients of the line fit are printed in each plot.

3.1   Centre of gravity and standard deviation of received power spectrum

The Figure 2 shows the evolution of the two parameters for each beam since the beginning of the ERS-2 mission and Figure 3 shows the same evolution only for the cycle 138.

The tendency during the nominal Yaw Steering Mode (YSM) period (beginning of the mission since the operation with the Mono Gyro (MGM) Attitude On-board Control System (AOCS) configuration on 7th February 2000) is a small and regular increase of the Centre of gravity (CoG) of received spectrum for the three antennae. During the YSM, two small changes can be detected in the CoG evolution. The first change is from 24th, January 1996 to 14th, March 1996, the second one is from 14th February 1997 to 22nd April 1997. The reason was a change in the pointing subsystem (DES reconfiguration) side B instead of side A after a depointing anomaly (see table 1 for the list of the all AOCS depointing anomaly occurred during the ERS-2 mission). During these periods side B was switched on. It is important to note that during the first time a clear difference in the CoG of the received spectrum is present only for the Fore antenna (an increase of roughly 100 Hz) while during the second time the change has affected all the three antennae (roughly an increase of 200 Hz, 50 Hz and

50 Hz for the fore, mid and aft antenna respectively).

At the beginning of 2000 the nominal 3-gyroes AOCS configuration (plus one Digital Earth Sensor -DES, and one Digital Sun Sensor -DSS and backups) was no more considered safe because 3 of the six gyros on-board were out of order or very noisy. For that reason the MGM was implemented as default piloting mode. The MGM configuration was designed to pilot the ERS-2 using only one gyro plus the DES and the DSS modules. Scope of ZGM configuration was to extend the satellite lifetime by using the available gyros one at the time.

With the MGM, an increase of roughly 200 Hz was observed at the end of the qualification period. After the AOCS commissioning phase this parameter further evolved within the nominal range with a negligible impact on the data quality.

In MGM configuration, the gyro 5 was used until 7th October 2000 when it failed. From 10th October 2000 to 24th October 2000 the gyro 6 was used. This explains the decrease of roughly 100Hz in the CoG of the received spectrum. From 25th October 2000 to 17th January 2001 the gyro 1 was used to pilot the ERS-2 satellite. On 17th January 2001 the AOCS was upgraded. The new configuration allows piloting the satellite without gyroscopes. Unfortunately a failure of the Digital Earth Sensor (DES A-side) caused ERS-2 to enter in Safe-Mode on the same day. On 25th January 2001 gyro #1 also failed.

Satellite attitude was recovered on 5th February 2001 with a coarse attitude control mode (EBM). During the period of safe mode the spacecraft had drifted out of the nominal dead band by some 30 Km. The nominal orbit was reached on 6th February 2001.
The EBM mode had a strong negative impact on the Scatterometer data quality and the dissemination of data products to end users was discontinued.

After that a series of AOCS upgrades has been implemented in order to improve the satellite attitude: on 30th March 2001 the Yaw steering law was re-introduced into the piloting function and on 7th June 2001 the Zero Gyro Mode (ZGM) has been implemented as nominal piloting mode. In ZGM the satellite attitude had an improvement in particular for the pitch and yaw error angle. This explains the reduction of the fluctuation in the received signal.

The CoG returns within its nominal value in February 2003 when the new ERS Scatterometer ground processor (ESACA) was put in operation (only for validation purposes) in Kiruna station. ESACA is able to compensate for errors in satellite attitude and to produce calibrated sigma noughts.

The evolution of the standard deviation of the CoG of the received spectrum was stable during the YSM phase. Small peaks are related with the events listed in Table 2. In MGM the evolution was within the nominal range while for the initial phase of the ZGM the performance was strong degraded. This because the on-ground Doppler filters was not able to compensate for the satellite degraded attitude. The introduction of the ESACA processor in February 2003 cured the problem.

On 8th December 2006 10:43 p.m. to 9th December 2006 07:18 anomaly in the on board Doppler Compensation occurred. That did not impact on the evolution of the CoG because the ESACA ground processor has compensated the receiver signal for the Doppler frequency shift. The Scat Team has carried out a deep analysis of the anomaly (see the technical note OSME-DPQC-SEDA-TN-06-0328 for further details).

TABLE 1 ERS-2 Scatterometer AOCS depointing anomaly list

Start of the anomaly			End of the anomaly			Remarks
24th January	1996	9:10 a.m.	26th January	1996	6:53 p.m.	AOCS depointing anomaly
14th February	1997	1:25 a.m.	15th February	1997	3:44 p.m.	AOCS depointing anomaly
3rd June	1998	2:43 p.m.	6th June	1998	12:47 a.m.	AOCS depointing anomaly
1st September	1999	8:50 a.m.	2nd September	1999	1:28 a.m.	
7th October	2000	4:38 p.m.	10th October	2000	4:49 p.m	depointing anomaly gyro 5 failure
24th October	2000	4:05 p.m.	25th October	2000	12:05 p.m.	depointing anomaly gyro 6 failure
17th January	2001		5th February	2001		gyro 1 failure Satellite in safe mode

TABLE 2 ERS-2 Scatterometer anomalies in the Doppler Compensation monitoring

Date start	Year	Date stop	Year	Reason
26th September	1996	27th September	1996	Missing on-board Doppler coefficient (after cal. DC converter test period)
6th June	1998	7th June	1998	No Yaw Steering Mode (after depointing anomaly)
2nd December	1998	3rd December	1998	Missing on-board Doppler coefficients (after AMI anomaly number 228)
16th February	2000	17th February	2000	Fine Pointing Mode (FPM) (due to AOCS mono-gyro qualification period)
14th April	2000	14th April	2000	Fine Pointing Mode (FPM)
5th July	2000	5th July	2000	Fine Pointing Mode (FPM) after instrument switch-on
27th September	2000	27th September	2000	Fine Pointing Mode (FPM) to upload AOCS software patch
2nd November	2000	2nd November	2000	Fine Pointing Mode (FPM)
5th December	2000	6th December	2000	Fine Pointing Mode (FPM) due to orbital manoeuvre
6th February	2001	30th March	2001	Extra Backup Mode (EBM) coarse attitude control

30th March	2001	17th June	2001	ZGM-EBM coarse attitude control
17th June	2001	21st August	2003	ZGM phase. Error in yaw angle not corrected in the ground segment processor. Data shall be reprocessed with ESACA.
24th March	2004	24th March	2004	Fine Pointing Mode (FPM) due to orbital manoeuvre
25th October	2004	27th October	2004	Series of orbital manoeuvres (OCM and FPM)
10th November	2004	11th November	2004	Intense geomagnetic storm
8th March	2005	8th March	2005	orbital manoeuvre (OCM)
11th March	2005	11th March	2005	orbital manoeuvre (FPM)
2nd November	2005	2nd November	2005	orbital manoeuvre (OCM)
1st March	2006	1st March	2006	orbital manoeuvre (OCM)
3rd November	2006	3rd November	2006	orbital manoeuvre (OCM) at 10:07:46
4th November	2006	4th November	2006	orbital manoeuvre (FCM) at 02:56:53 and 04:37:38
8th December	2006	9th December	2006	Missing on-board Doppler coefficients after AMI anomaly from 10:43 p.m. to 9th December 2006 07:18 a.m.
19th December	2006	19th December	2006	orbital manoeuvre (FCM) at 23:06:12
1st February	2007	1st February	2007	orbital manoeuvre (FCM) at 02:53:31
13th February	2007	13th February	2007	orbital manoeuvre (FCM) at 05:00:15 and 06:40:51
14th February	2007	14th February	2007	orbital manoeuvre (OCM) at 09:30:29
26th April	2007	26th April	2007	Orbital manoeuvre (FCM) at 03:12:03
11th May	2007	11th May	2007	Orbital manoeuvre (FCM) at 02:04:10
13th June	2007	13th June	2007	Orbital manoeuvre (FCM) at 03:41:38
10th September	2007	10th September	2007	Orbital manoeuvre (FCM) at 02:10:29 and 03:51:05
11th September	2007	11th September	2007	Orbital manoeuvre (FCM) at 10:01:58
12th September	2007	12th September	2007	Orbital manoeuvre (FCM) at 02:47:55 and 04:28:31
13th September	2007	13th September	2007	Orbital manoeuvre (FCM) at 05:37:30 and 07:18:16
14th September	2007	14th September	2007	Orbital manoeuvre (OCM) at 10:07:42
15th September	2007	15th September	2007	Orbital manoeuvre (FCM) at 23:00:51
16th September	2007	16th September	2007	Orbital manoeuvre (FCM) at 00:41:27
18th October	2007	18th October	2007	Orbital manoeuvre (FCM) at 02:00:00
30th October	2007	30th October	2007	Orbital manoeuvre (FCM) at 02:03:10
16th November	2007	16th November	2007	Orbital manoeuvre (FCM) at 02:51:08
4th December	2007	4th December	2007	Orbital manoeuvre (FCM) at 02:39:54
4th December	2007	4th December	2007	Orbital manoeuvre (FCM) at 04:20:30
7th December	2007	7th December	2007	Orbital manoeuvre (FCM) at 16:10:00
19th December	2007	19th December	2007	Orbital manoeuvre (FCM) at 01:28:00
10th January	2008	10th January	2007	Orbital manoeuvre (FCM) at 02:00:00

31st January	2008	31st January	2008	Orbital manoeuvre (FCM) at 03:30:45
14th February	2008	14th February	2008	Orbital manoeuvre (FCM) at 02:58:12
7th March	2008	7th March	2008	Orbital manoeuvre (FCM) at 03:00:00
20th March	2008	20th March	2008	Orbital manoeuvre (FCM) at 02:58:21
30th May	2008	30th May	2008	Orbital manoeuvre (FCM) at 01:45:00
30th May	2008	30th May	2008	Orbital manoeuvre (FCM) at 02:35:14

The Doppler compensation evolution for cycle 138 is showed in Figure 3. The monitoring shows a daily average of the CoG of the compensated received signal around 30 Hz and -80 Hz for the Fore and Aft antenna respectively. For the Mid antenna it was around 240 Hz. The standard deviation of the CoG was around 1500 Hz for the Fore and Aft antenna and around 2750 Hz for the Mid antenna. Those values are within the nominal range.

ERS-2 WindScatterometer: DOPPLER COMPENSATION Evolution (UWI)

Least-square poly. fit fore beam   Center of gravity = -13.38 +(0.0091)*day   Standard Deviation = 5290.6 +(-0.902)*day
Least-square poly. fit mid beam   Center of gravity = -691.4 +(0.2427)*day   Standard Deviation = 5936.1 +(-0.768)*day
Least-square poly. fit aft beam   Center of gravity = -266.2 +(0.0722)*day   Standard Deviation = 5434.7 +(-0.935)*day
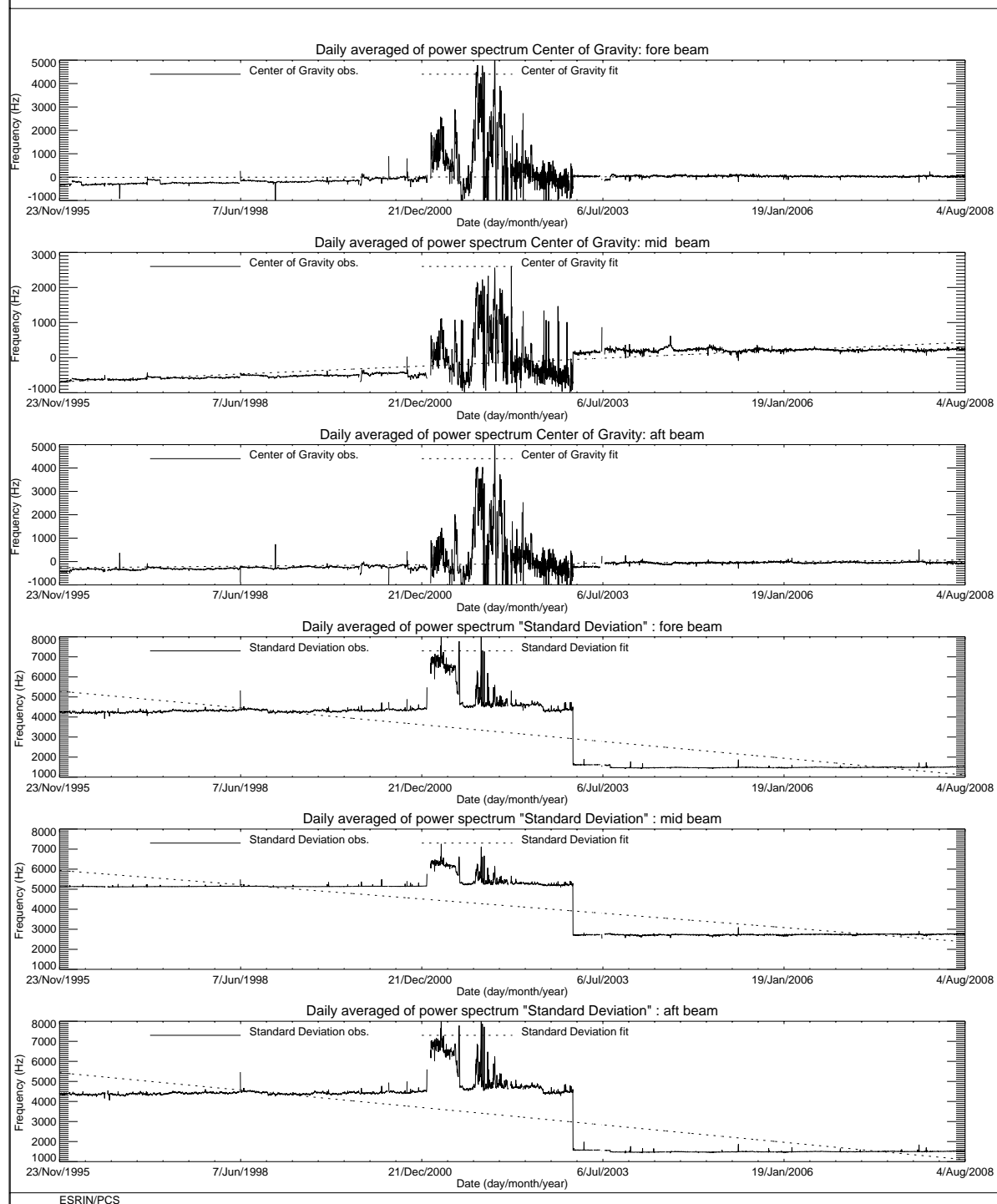

ESRIN/PCS

FIGURE 2 ERS-2 Scatterometer: Centre of Gravity and standard deviation of received power spectrum since the beginning of the mission.

16

ERS-2 WindScatterometer: DOPPLER COMPENSATION Evolution (UWI)

Least-square poly. fit fore beam   Center of gravity = 31.917 +(0.0090)*day Standard Deviation = 1509.3 +(0.0831)*day
Least-square poly. fit mid beam   Center of gravity = 236.31 +(0.1569)*day Standard Deviation = 2763.4 +(-0.022)*day
Least-square poly. fit aft beam   Center of gravity = -79.72 +(0.2932)*day Standard Deviation = 1517.2 +(0.1392)*day
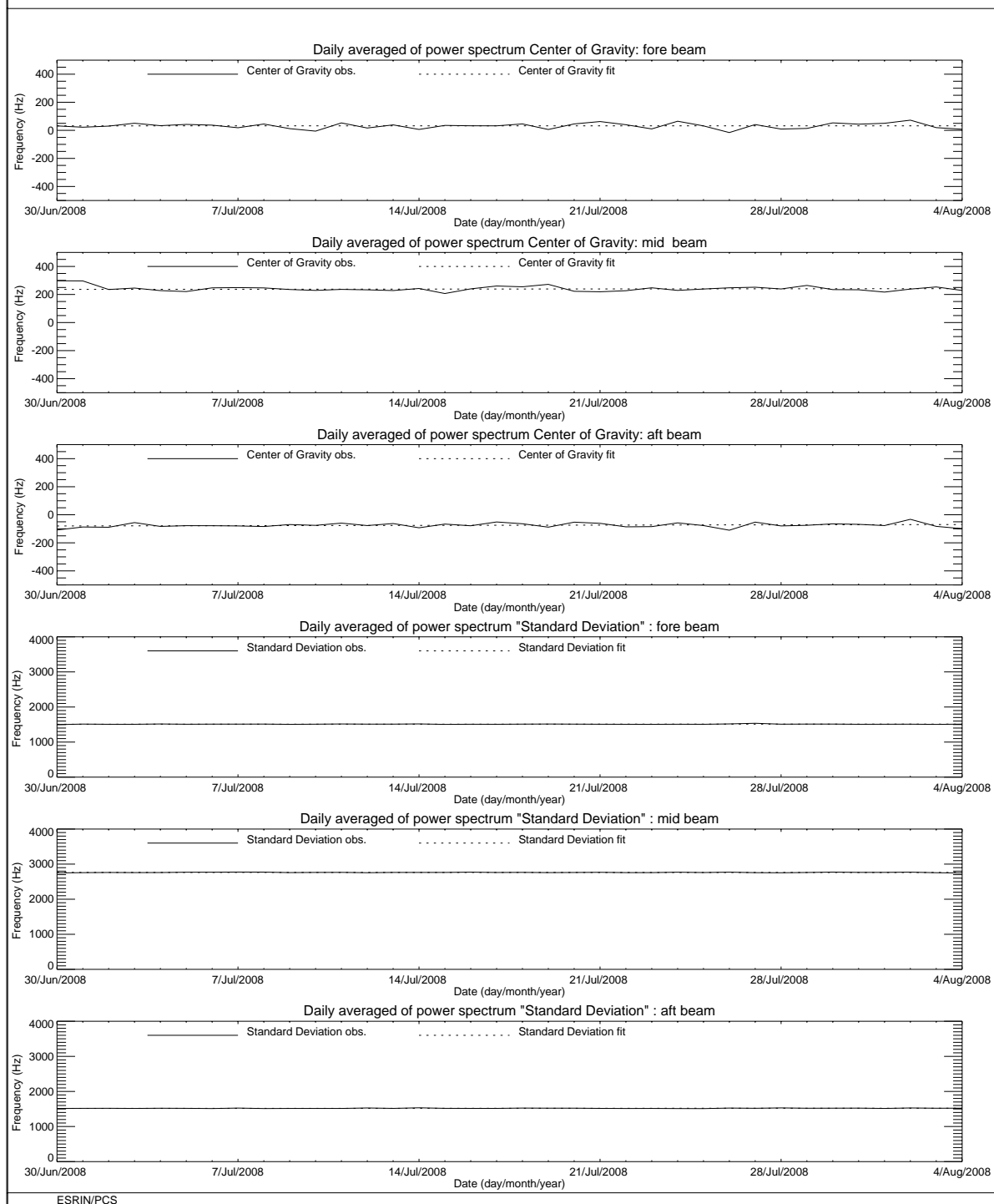

FIGURE 3 ERS-2 Scatterometer: Centre of Gravity and standard deviation of received power spectrum for cycle 138.

3.2   Noise power level I and Q channel

The results of the monitoring are shown in Figure 4 (long-term) and Figure 5 (cycle 138). The first set of three plots presents the noise power evolution for the I channel while the second set shows the Q channel. From the plots one can see that the noise level is more stable in the I channel than in the Q one. The I and Q receivers are inside the same box and any external interference should affect both channel. The fact that the receivers are closer to the ATSR-GOME electronics could have some impact but there is no clear explanation on that behavior. From 5th December 1997 until November 1998 some high peaks appear in the plots. These high values for the daily mean are due to the presence for these special days of a single UWI product with an unrealistic value in the noise power field of its Specific Product Header. The analysis of the raw data used to generate these products lead in all cases to the presence of one source packet with a corrupted value in the noise field stored into the source packet Secondary Header. The reason why noise field corruption is beginning from 5th December 1997 and last until November 1998 is at present unknown. It is interesting to note that at the beginning of December 1997, we started to get as well the corruption of the Satellite Binary Times (SBTs) stored in the EWIC product. The impact in the fast delivery products was the production of blank products starting from the corrupted EWIC until the end of the scheduled stop time. A change in the ground station processing in March 1998 overcame this problem.

Since 9th August 1998 until March 2000 some periods with a clear small instability in the noise power have been recognized, Table 3 gives the detailed list.

TABLE 3 ERS-2 Periods with instability in the noise power

Start date	Stop date	Year
9th August	26th October	1998
29th November	6th December	1998
23rd December	24th December	1998
7th June	10th June	1999
17th August	22nd August	1999
8th September	9th September	1999
3rd October	8th October	1999
16th October	18th October	1999
26th October	28th October	1999
25th December	2nd January	2000
10th February	11th February	2000
19th March	26th March	2000

To better understand the instability of the noise power the PCS has carried out investigations in the Scatterometer raw data (EWIC) to compute the noise power with more resolution. The result is that for the orbits affected by the instability the noise power had a decrease of roughly 0.7 dB for the fore and aft signals and a decrease of roughly 0.6 dB in the mid beam case (see the report for the cycle 42). The decrease of the noise power during the orbits affected by the instability is comparable with the decrease of the internal calibration level that occurred during the same orbits. The reason of this instability (linked to the AMI anomalies) is still unknown. On 28th February 2003 the Scatterometer receiver gain has been increased by 3 dB to optimize the usage of the on-board ADC converter. This explains the increase of the noise for the Fore and Aft beam channel. For the mid beam channel the noise still remains not measurable.

On 17th February 2006 a high peak was detected in the noise power, causing the daily average for that day very high. The case has been deeply investigated and a technical note (Ref OSME-DPQC-SEDA-TN-06-0163) is available. The cause was an acquisition problem that corrupted one source packet and not an instrument anomaly. The same happened on April 24th 2006 (cycle 115).

On 8th September 2006 a high peak in the noise power of the Mid beam has been detected. The event occurred between 17:41:54 and 17:42:43 (UTC) and the noise power reached the value of 43 ADC (fore beam) and 19 ADC (mid beam). Those values had affected the daily average and are clear present in the plots of the Figure 4. That anomaly has been deeply investigated in the Technical Note OSME-DPQC-SEDA-TN-06-0251 and cannot be linked to any anomaly in the acquired data. The conclusion of the investigation was that a problem had occurred in the transmitter or in the pulse generator of the AMI instrument. At that time the AMI was in wind only mode so no additional comparison with SAR data can be done. Similar peaks had been noted also for September 15th and 18th. ESOC has checked the Mission Plan and noticed that in all three events the peak in the noise power occurred very close to 6 minutes after the start of a Wind mode and 40 minutes after ascending node crossing.

The evolution of the noise power during the cycle 138 was stable. The daily average for the Fore and Aft beam noise is around 1.7 ADC (I) and around 1.6 ADC (Q) respectively. For the Mid beam the noise is not measurable. During the reporting period many orbits with peaks in the noise power have been detected. Investigations are on-going.

ERS-2 WindScatterometer: NOISE Level Evolution (UWI)

Least-square line fit fore beam: I = 748.29 +(0.2384)*day   Q = 697.40 +(0.2257)*day

I channel: No line fit standard deviation too hight   Q channel: No line fit standard deviation too hight

Least-square line fit aft beam: I = 746.81 +(0.2289)*day   Q channel: No line fit standard deviation too hight
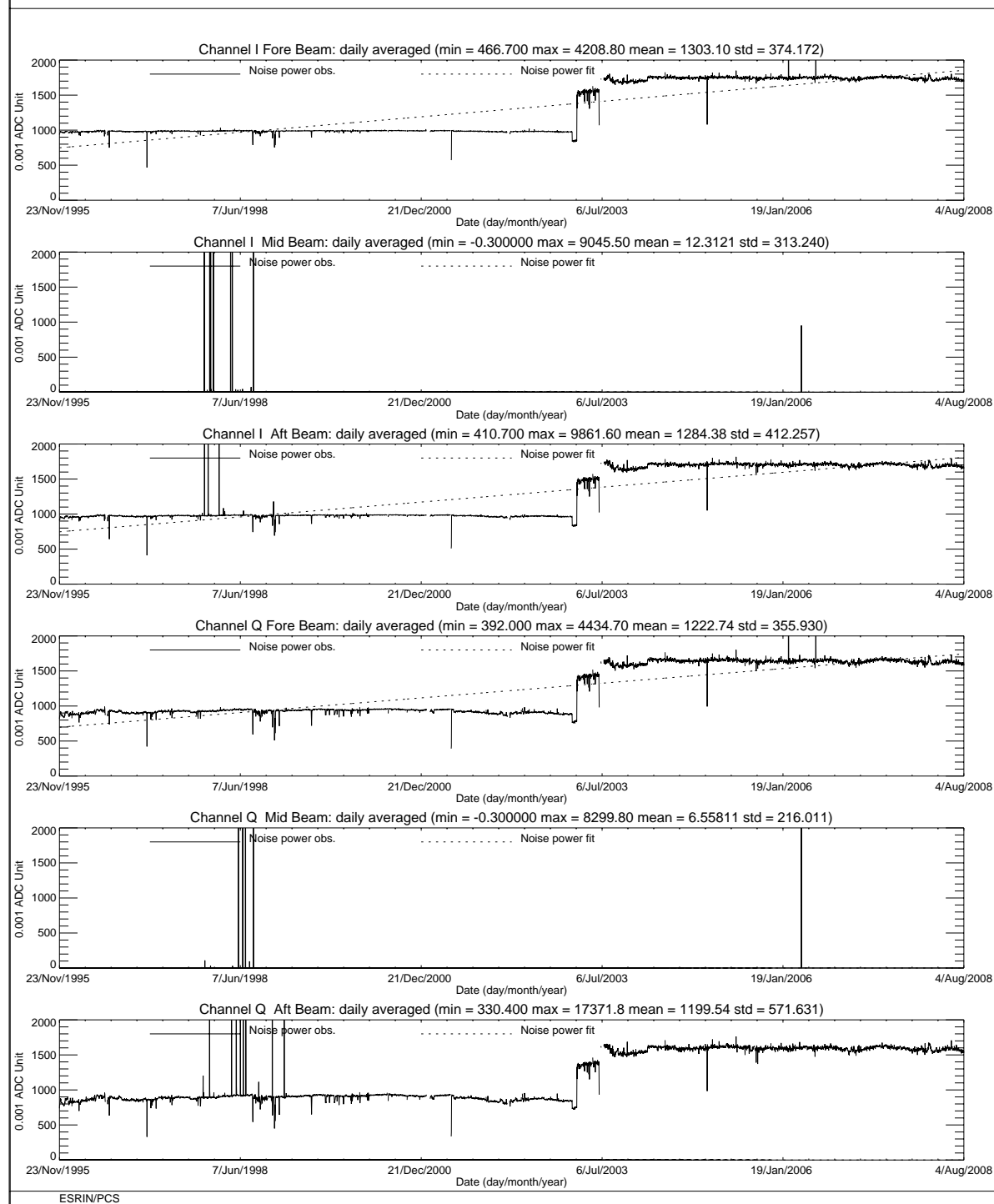
Channel I Fore Beam: daily averaged (min = 466.700 max = 4208.80 mean = 1303.10 std = 374.172)

Channel I Mid Beam: daily averaged (min = -0.300000 max = 9045.50 mean = 12.3121 std = 313.240)

Channel I Aft Beam: daily averaged (min = 410.700 max = 9861.60 mean = 1284.38 std = 412.257)

Channel Q Fore Beam: daily averaged (min = 392.000 max = 4434.70 mean = 1222.74 std = 355.930)

Channel Q Mid Beam: daily averaged (min = -0.300000 max = 8299.80 mean = 6.55811 std = 216.011)

Channel Q Aft Beam: daily averaged (min = 330.400 max = 17371.8 mean = 1199.54 std = 571.631)

ESRIN/PCS

FIGURE 4 ERS-2 Scatterometer: noise power I and Q channel since the beginning of the mission.

ERS-2 WindScatterometer: NOISE Level Evolution (UWI)

Least-square line fit fore beam:	I = 1731.2 +(-0.713)*day	Q = 1627.4 +(-0.971)*day
Least-square line fit mid beam:	I = 0.0296 +(0.0030)*day	Q = -0.025 +(0.0079)*day
Least-square line fit aft beam:	I = 1692.4 +(-0.908)*day	Q = 1580.5 +(-1.130)*day

ESRIN/PCS
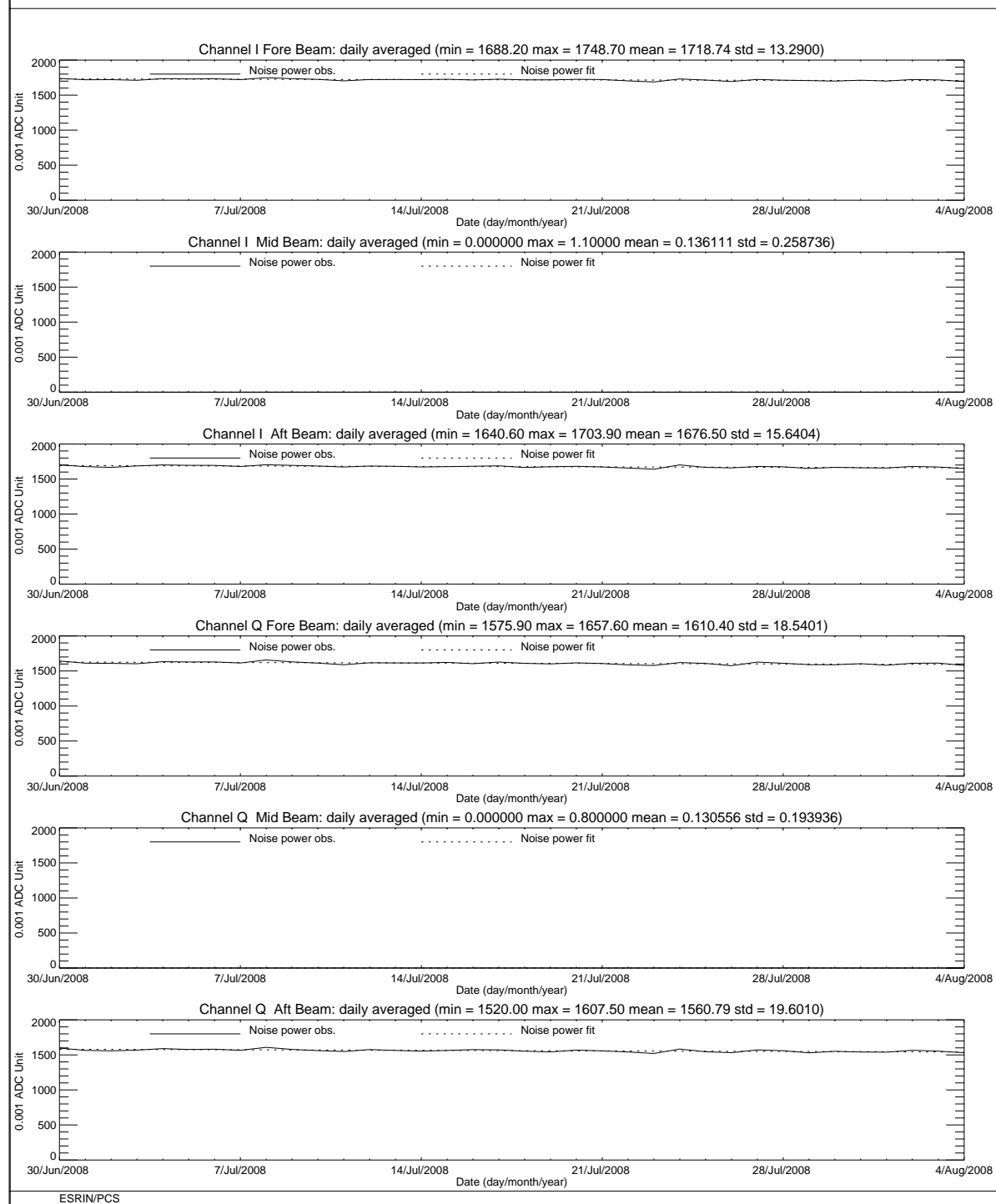
FIGURE 5 ERS-2 Scatterometer: noise power I and Q channel for cycle 138.

3.3 Power level of internal calibration pulse

For the internal calibration level, the results are shown in Figure 6 (long-term) and Figure 7 (cycle 138). The high value of the variance in the fore beam until August, 12th 1996 is due to the ground processing. In fact all the blank source packets ingested by the processor were recognized as Fore beam source packets with a default value for the internal calibration level. The default value was applicable for ERS-1 and therefore was not appropriate for ERS-2 data processing. On August 12th, 1996 a change in the ground processing LUT overcame the problem. Since the beginning of the mission a power decrease is detected. The power decrease is regular and affects the AMI when it is working in wind-only mode, wind/wave mode and image mode indifferently. The average power decrease is around 0.08 dB per cycle (0.0022 dB/day) and is clearer after August, 6th 1996 when the calibration subsystem has been changed. The reason of the power decrease is because the TWT is not working in saturation, so that a variation in the input signal is visible in the output. The variability of the input signal can be two-fold: the evolution of the pulse generator or the tendency of the switches between the pulse generator and the TWT to reset themselves into a nominal position. These switches were set into an intermediate position in order to put into operation the Scatterometer instrument (on 16th November 1995). To compensate for this decrease, on 26th October 1998 (cycle 37) 2.0 dB were added to the Scatterometer transmitted power and on 4th September 2002 (cycle 77) were added 3.0 dB. On 28th February 2003 (cycle 82) the Scatterometer receiver gain was increased by 3 dB to improve the usage of the on-board ADC converter. These events are clearly displayed by the large steps show in Figure 6.

Since 9th August 1998 until March 2000 the internal calibration level shows instability after an AMI or platform anomaly (see reports from cycle 35 to cycle 52). This instability is very well correlated with the fluctuations observed in the noise power. On 13th July 2000 a high peak (+3.5 dB) was detected in the transmitted power. This event has been investigated deeply by PCS and ESOC. The results of the analysis are reported in the technical note "ERS-2 Scatterometer: high peak in the calibration level" available in the PCS. The high transmitted power was detected after an arcing event which occurred inside the HPA. After that event the transmitted power had an average increase of roughly 0.14 dB.

During the cycle 138 the mean transmitted power evolution had a mean decrease of 0.11 dB. This value is similar to the nominal decreasing trend of 0.1 dB/Cycle detected since the beginning of the mission. This parameter will be further monitored in the next cycles.

ERS-2 WindScatterometer: Internal CALIBRATION Level Evolution (UWI)

Least-square polynomial fit fore beam	gain (dB) per day 0.0000	1051.59 +(-0.00308691)*day
Least-square polynomial fit mid beam	gain (dB) per day 0.0000	311.941 +(-0.00137886)*day
Least-square polynomial fit aft beam	gain (dB) per day 0.0000	1040.56 +(-0.00261155)*day
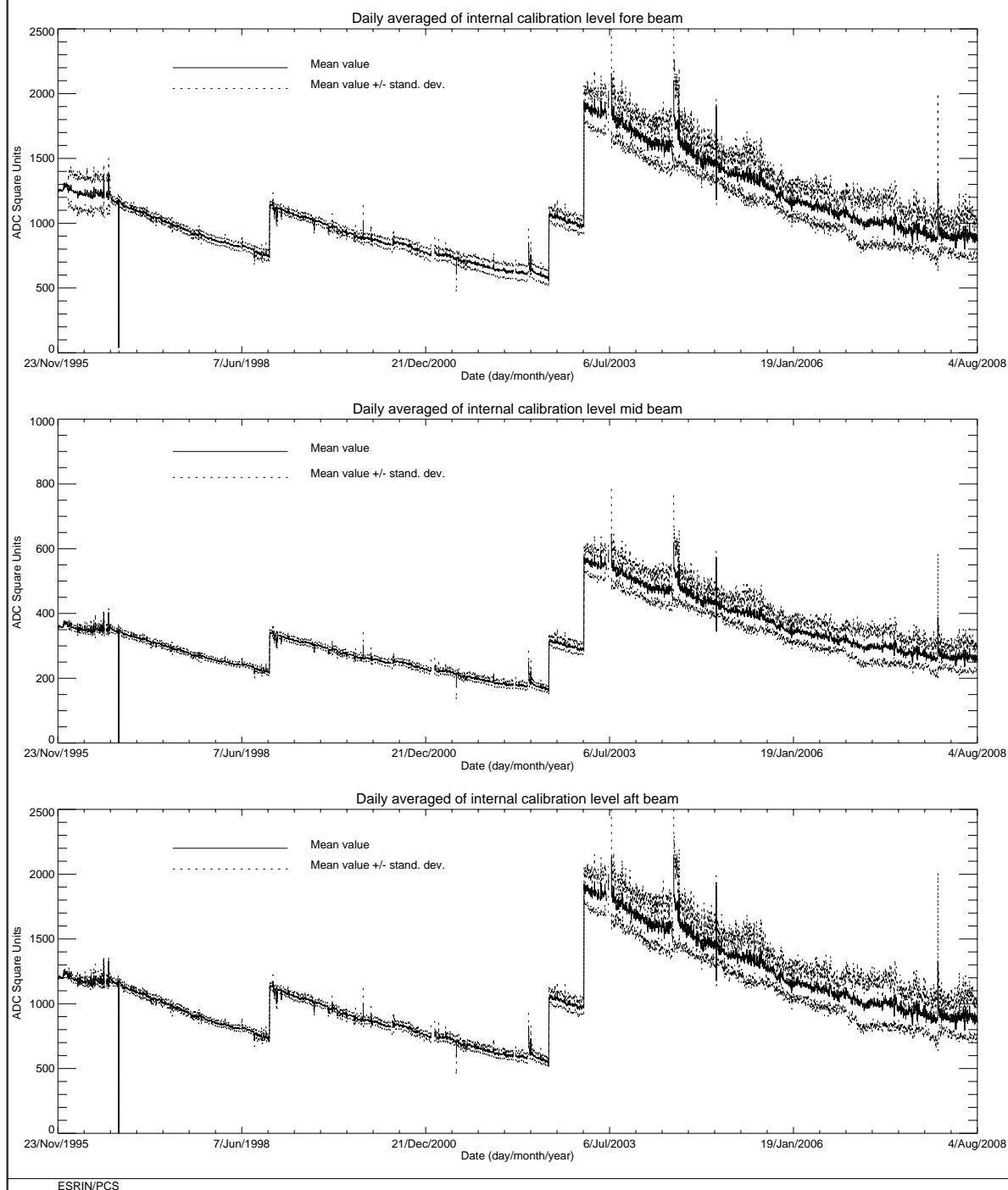
FIGURE 6 ERS-2 Scatterometer: power of internal calibration pulse since the beginning of the mission.

ERS-2 WindScatterometer: Internal CALIBRATION Level Evolution (UWI)

Least-square polynomial fit fore beam	gain (dB) per day -0.0031	901.168 +(-0.630130)*day
Least-square polynomial fit mid beam	gain (dB) per day -0.0031	265.510 +(-0.189410)*day
Least-square polynomial fit aft beam	gain (dB) per day -0.0034	898.508 +(-0.692824)*day

ESRIN/PCS
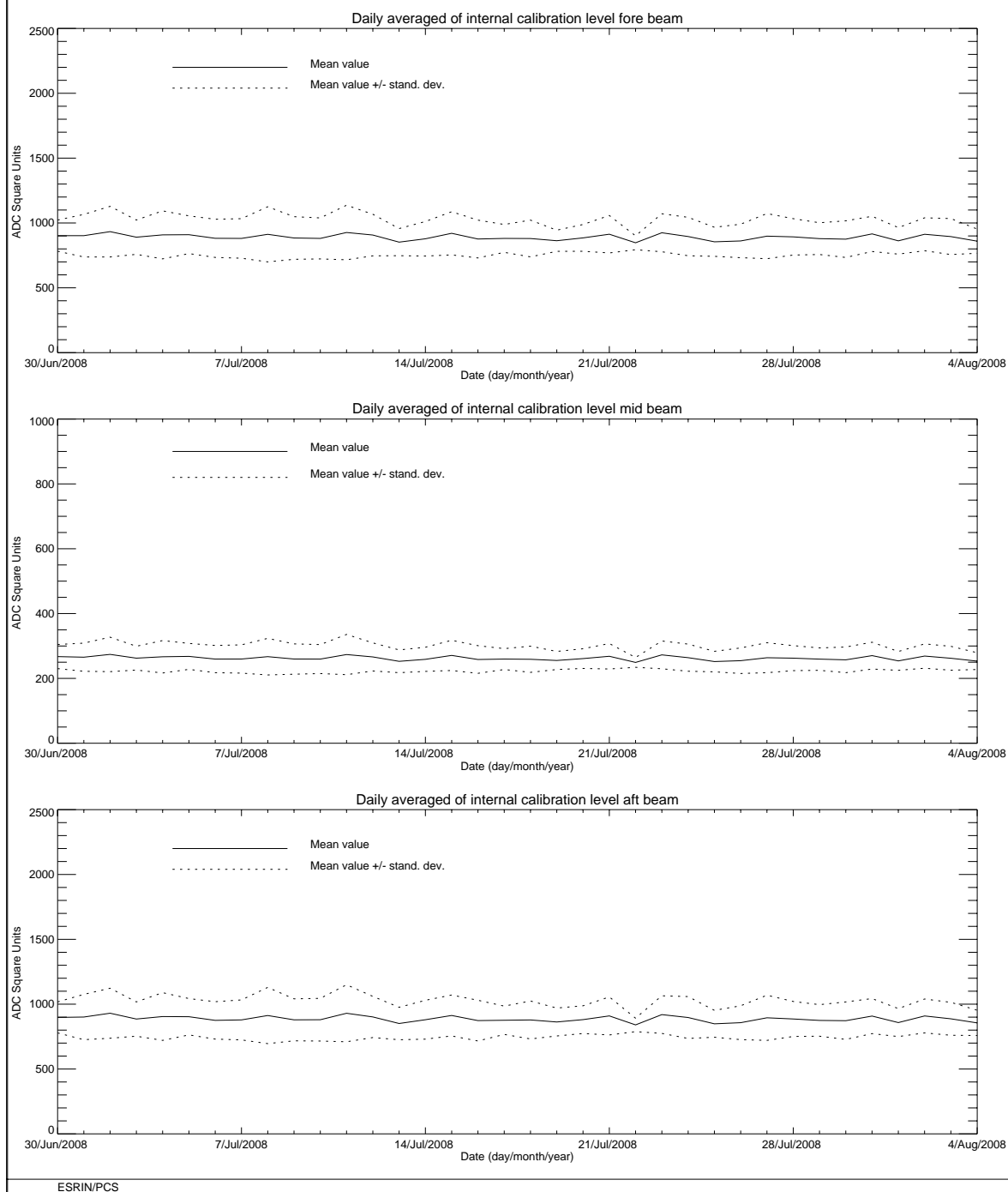
FIGURE 7 ERS-2 Scatterometer: power of internal calibration level cycle 138.

4   <u>Products performance</u>

The PCS carries out a quality control of the winds generated from the WSCATT data. External contributions to this quality control (from ECMWF) are also reported in this chapter.

4.1   Products availability

One of the most important points in the monitoring of the products performance is their availability. The Scatterometer is a part of ERS payload and it is combined with a Synthetic Aperture Radar (SAR) into a single Active Microwave Instrument (AMI). The SAR users requirements and the constraints imposed by the on-board hardware (e.g. amount of data that can be recorded in the on-board tape) set rules in the mission operation plan.

The principal rules that affected the Scatterometer instrument data coverage are:
• Over the Ocean the AMI is in wind/wave mode (Scatterometer with small SAR imagettes acquired every 30 sec.) and the ATSR-2 is in low rate data mode.
• Over the Land the AMI is in wind only mode (only Scatterometer) and the ATSR-2 is in high rate mode. (Due to on board recorder capacity, ATSR-2 in high rate is not compatible with SAR wave imagettes acquisitions.) This strategy preserves the Ocean mission.
• The SAR images are planned as consequence of users' request.

Moreover:
- since July 16th 2003 the ERS-2 Low Rate mission is continued within only the visibility of ESA ground stations over Europe, North Atlantic, the Arctic and western North America. The reason was the failure of both on-board tape recorders.
- During the cycles 64 – 92 (June 2001 since 25th February 2004) the AMI instrument was operated in wind/wave mode also over the land. The reason was because the SAR wave data was used to estimate the satellite mispointing along the full orbit. Since 25th February onwards the nominal mission scenario has been resumed, with the AMI instrument in wind only mode over the land (and consequently ATSR was operated again in High Rate over land). The mispointing performances (in particular the yaw error angle) along the full orbit are computing by analyzing the Scatterometer data.

In order to maximize the data coverage, after the on-board tape recorder failure, an upgrade of the ERS ground segment acquisition scenario has been performed.
In that framework the following has been implemented:

- Since September 7th 2003 the ground station in Maspalomas, Gatineau and Prince Albert are acquiring and processing data for all the ERS-2 satellite passes within the station visibility (apart from passes for which other satellites have an higher priority).

- To further increase the wind coverage of the North Atlantic area, since December 8th, 2003 is operative a new ground Station in West Freugh (UK) and data from this new station are available to the user since mid January 2004. Due to its location, the West Freugh acquisitions have some overlap with those from three other ESA stations, Kiruna, Gatineau or Maspalomas. The station overlap depends on the relative orbit of the satellite. Consequentially, overlapping wind Scatterometer LBR data may be included in two products. Since the two products are generated at different ground stations the overlap may not be completely precise, with a displacement up to 12 Km and slight differences in the wind data itself.

- Since March, 3rd 2004, Matera station is acquiring and processing low rate bit data for all the passes for which is planned a SAR acquisition. This means for the Scatterometer data coverage a limited improvement due to the fact that is acquired only a passage with some planned SAR activity.

- Since February 2005 a new acquisition station in Miami (US) is in operations. This new station allows a full data coverage of the Gulf of Mexico and part of the Pacific Ocean on the west Mexico coast.

- Since 25th, June 2005 a new acquisition stations have been put into operations in Beijing. It covers part of China and Oriental Asia.

- Since 5th July 2005 McMurdo ground station is operational in the South Pole. It covers all the Antarctic region.

- Since 5th December 2005 the Hobart station is operational and it is covering the Australian and New Zealand area. Hobart data has been disseminated into BUFR format since February 13th 2006.

- At the end of August 2006 a new ground station in Singapore has been installed and products are distributed to the users since October 19th 2006.

- At the end of September 2007 a new ground station has been put into operation in Chetumal (Mexico). Products are distributed to the users since October 18th 2007.

- On May 2008 a new ground station is operational in Johannesburg. Data has been disseminated to users since July 2008.

Figure 8 shows the AMI operational modes for cycle 138. Each segment of the orbit has different color depending on the instrument mode: brown for wind only mode, blue for wind-wave mode and green for image mode. The red and yellow colors correspond to gap modes (no data acquired). For cycle 138 the percentage of the ERS-2 AMI activity is shown in table

4. The value for cycle 138 shows an increase of SAR activity at descending passes with respect to the cycle 137 (17.29%, was 15.09%).

TABLE 4 ERS-2 AMI activity (cycle 138)

Ami Mode	Ascending passes	Descending passes
Wind and Wind-Wave	**87.42 %**	**74.80%**
Image	**4.59 %**	**17.29 %**
Gap and others	**7.98 %**	**7.9 %**

Table 5 reports the major data lost (day or more) due to the test periods, AMI and satellite anomalies or ground segment anomalies occurred after 6th August, 1996 (before that day for many times data were not acquired due to the DC converter failure).

TABLE 5 ERS-2 Scatterometer mission major data lost (day or more) after 6th, August 1996

Start date	Stop Date	Reason
September 23rd, 1996	September 26th, 1996	ERS 2 switched off due to a test period
February 14th, 1997	February 15th, 1997	ERS 2 switched off due to a depointing anomaly
June 3rd, 1998	June 6th, 1998	ERS 2 switched off due to a depointing anomaly
November 17th, 1998	November 18th, 1998	ERS 2 switched off to face out Leonide meteor storm
September 22nd 1999	September 23rd 1999	ERS 2 switched off due to Year 2000 certification test
November 17th, 1999	November 18th, 1999	ERS 2 switched off to face out Leonide meteor storm
December 31st, 1999	January 2nd, 2000	ERS 2 switched off Y2K transition operation
February 7th, 2000	February 9th, 2000	ERS 2 switched off due to new AOCS s/w up link
June 30th, 2000	July 5th, 2000	ERS 2 Payload switched off after RA anomaly
July 10th, 2000	July 11th, 2000	ERS 2 Payload reconfiguration
October 7th, 2000	October 10th 2000	ERS 2 Payload switched off after AOCS anomaly
January 17th, 2001	February 5th, 2001	ERS 2 Payload switched off due to AOCS anomaly
May 22nd, 2001	May 24th, 2001	ERS 2 Payload switched off due to platform anomaly
May 25th, 2001	May 25th, 2001	AMI switched off due thermal analysis
November 17th, 2001	November 18th, 2001	ERS 2 switched off to face out Leonide meteor storm
November 27th, 2001	November 28th, 2001	ERS 2 payload off due to 1Gyro Coarse Mode commissioning
March 8th, 2002	March 20th, 2002	ERS 2 payload unavailability after RA anomaly
May 19th, 2002	May 24th 2002	AMI switched off due to arc events
May 24th, 2002	May 28th, 2002	AMI partially switched off due to arc events
May 31st 2002	June 3rd 2002	Gatineau orbits partially acquired due to antenna problem
June 4th, 2002	June 5th, 2002	AMI partially switched-off due to arc events

July 25th, 2002	July 25th, 2002	AMI switched off HPA voltage too low
September 11th, 2002	September 11th, 2002	AMI switched off macrocommand transfer error
November 17th, 2002	November 18th, 2002	ERS-2 switched off to face out Leonide meteor storm
December 9th, 2002	December 10th, 2002	IDHT anomaly no data recorded on board
December 20th, 2002	December 20th 2002	IDHT anomaly no data recorded on board
January 14th, 2003	January 14th, 2003	IDHT anomaly no data recorded on board
May 6th, 2003	May 19th, 2003	AMI off due to bus reconfiguration
June 22nd, 2003	July 16th, 2003	IDHT recorders test no data acquired
Since July 16th, 2003		Regional Mission Scenario. Data available only within the visibility of ESA ground station
May 21st, 2004	May 25th, 2004	AMI in refuse mode due to excessive HPA arcing
June 22nd, 2004	June 22nd, 2004	AMI in refuse mode due to excessive HPA arcing
September 23rd, 2004	September 24th, 2004	AMI switched down
December 16th, 2004	December 17th, 2004	AMI memory test
December 26th, 2004	December 26th, 2004	IDHT anomaly. No data acquired
December 27th, 2004	December 28th, 2004	Payload off due to on board anomaly
January 23rd, 2005	January 23rd, 2005	AMI switched down (00.51 a.m. – 1.26 p.m.)
February 26th, 2005	February 26th, 2005	AMI switched down (01.20 a.m. – 12.37 a.m.)
May 23rd, 2005	May 24th, 2005	ERS 2 payload unavailability after RA anomaly
Jun 20th, 2005	Jun 21st, 2005	AMI switched off caused by RBI status error (08:44 p.m. – 10:13 a.m.)
December 8th, 2006	December 8th, 2006	AMI switched down to Standby/MCMD Execution Inhibited due to Format Acquisition Error (02:04 p.m. – 10:43 p.m.)
April, 13th, 2007	April 13th, 2007	AMI Switched down to Standby/MCMD Execution Inhibited due to Format Acquisition Error (03:10 a.m. – 12.06 p.m.)
May, 22nd, 2007	May, 22nd, 2007	AMI Switched down to Standby/MCMD Execution Inhibited due to Acquisition Errors (01:50 p.m. – 07.04 p.m.)
June, 10th, 2007	June, 10th, 2007	AMI Switched down to Standby/MCMD Execution Inhibited due to Format Length and ICU Begin Identifier Errors (00:55 a.m. – 10.13 a.m.)
June, 11th, 2007	June, 12th, 2007	AMI Switched down to Standby/MCMD Execution Inhibited due to Emergency Switchdown requested by AMI ICU (10:39 p.m. – 10.49 a.m.)
July, 27th, 2007	July, 27th, 2007	AMI switchdown to Standby/MCMD Execution Inhibited due to RBI Status Error (00:44 a.m. - 09:43 a.m).
January, 17th, 2007	January, 17th, 2007	AMI switched down to Heater/MCMD Refuse mode due to HPA Arcing (04:01 a.m. – 07:22 p.m.)
January, 17th, 2007	January, 18th, 2007	AMI switched down to Heater/MCMD Refuse mode due to HPA Arcing (07:51 p.m. – 12:49 p.m.)
January, 18th, 2007	January, 18th, 2007	AMI switched down to Heater/MCMD Refuse mode due to HPA Arcing (03:26 p.m. – 03:39 p.m.)
January, 18th, 2007	January, 18th, 2007	AMI switched down to Heater/MCMD Refuse mode due to HPA Arcing (08:12 p.m. – 08:31 p.m.)
January, 18th, 2007	January, 19th, 2007	AMI switched down to Heater/MCMD Refuse mode due to HPA Arcing (10:37 p.m. – 01:32 a.m.)
January, 20th, 2007	January, 20th, 2007	AMI switched down to Heater/MCMD Refuse mode due to HPA Arcing (02:04 a.m. – 07:53 a.m.)

February, 5th, 2007	February, 5th, 2007	AMI switched down to Standby/MCMD Execution Inhibited due to Format Length and ICU Begin Identifier Errors (02:05:09 a.m. – 05:43:33 p.m.)
February, 6th, 2007	February, 6th, 2007	AMI switched down to Standby/MCMD Execution Inhibited due to Format Length and ICU Begin Identifier Errors (12:14:23 p.m. – 12:52:51 p.m.)
April, 14th, 2008	April, 14th, April	AMI switched down to Standby/MCMD Execution Inhibited due to Format Length and ICU Begin Identifier Errors (13:43:34 – 18:57:19)
April, 30th, 2008	April, 30th, 2008	AMI switched down to Standby/MCMD Refuse Mode due to 228 ICU Req. (08:25:42 – 11:44:05)
June, 12th, 2008	June, 12th, 2008	AMI switched down to Heater/MCMD Refuse Mode due to incorrect timetag entered for quarterly AMI Science Data Memory Test (08:44:43 – 09:10:34)
June, 16th, 2008	June, 12th, 2008	AMI Switched down to Standby/MCMD Execution Inhibited due to Format Length and ICU Begin Identifier Errors (01:17:26 – 10:24:10).
June, 20th, 2008	June, 20th, 2008	AMI Emergency Switchdown to Standby/MCMD Execution Inhibited due to RBI Status Error (13:12:22 – 18:20:40).
June, 29th, 2008	June, 29th, 2008	AMI unavailable for PL Synchronisation (20:23:00 – 20:48:59)
July, 26th, 2008	July, 26th, 2008	AMI in Standby/MCMD Refused due to Anomaly 228 ICU REQ 1500 0082 (18:38:30 – 22:40:52)

ERS-2 Active Microwave Instrument: Working modes

First product : 30/Jun/2008 0:00:03.523   Last product : 3/Aug/2008 23:59:47.564

Products found: 61311   Created   : 05-AUG-2008 10:12:50.000

Cylindrical projection: Descending passes
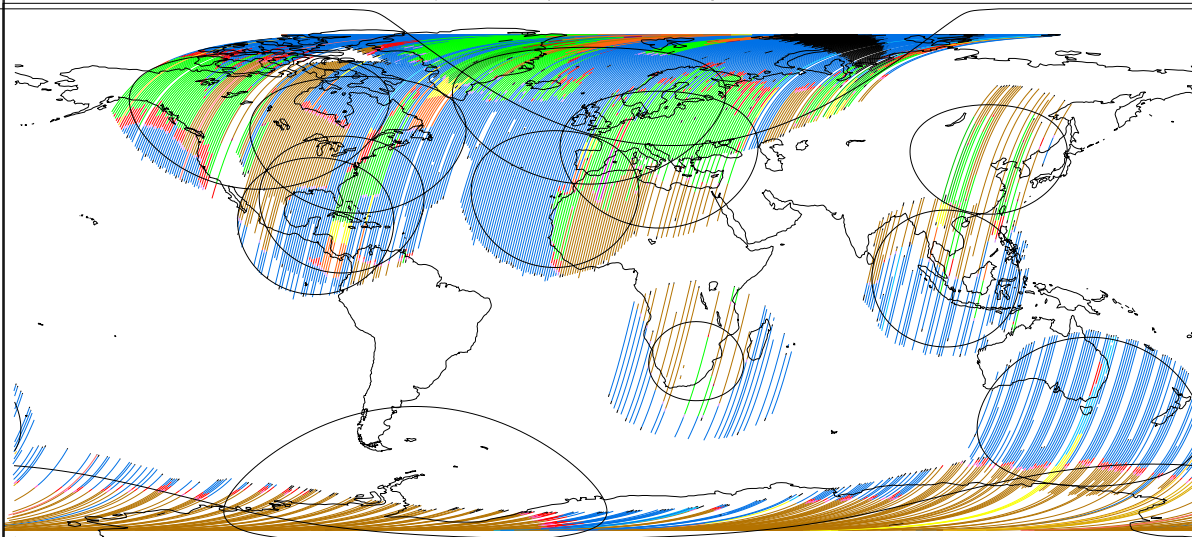
Cylindrical projection: Ascending passes
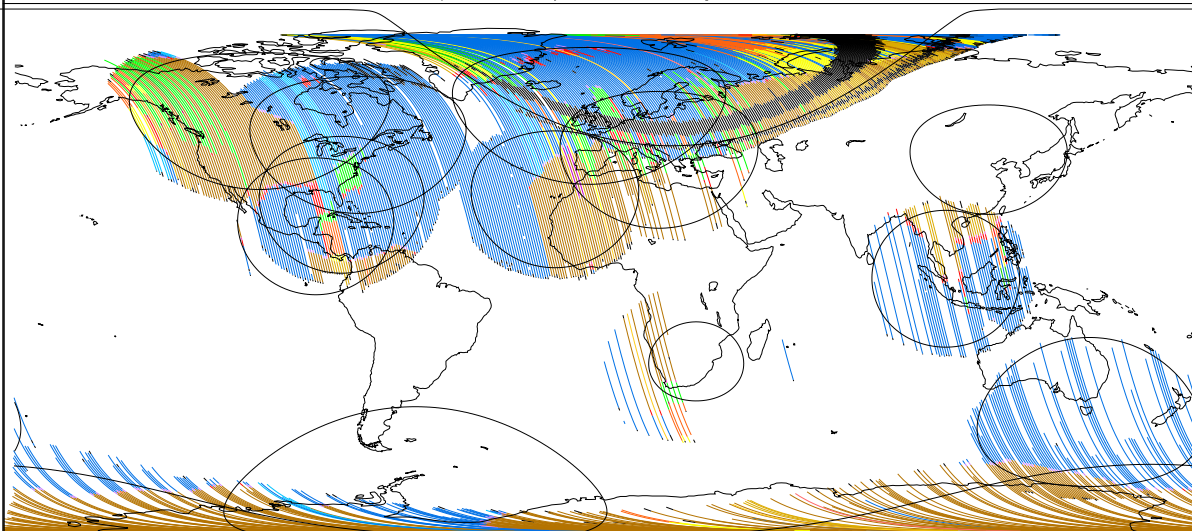
AMI MODE Decoding Key and percentage of occurences per mode & passage

Mode	A / D values
WI/WV OG HTR	A 0.000 D 0.000
WI/WV OB GAP	A 46.34 D 45.86
WI/WV OB HTR	A 2.350 D 0.840
WIND CAL GAP	A 0.120 D 0.110
WIND CAL HTR	A 0.000 D 0.000
HEATER	A 2.330 D 1.140
GAP	A 1.220 D 3.010
IMAGE OB HTR	A 0.000 D 0.000
WAVE OG GAP	A 0.000 D 0.000
WAVE OG HTR	A 0.000 D 0.000
WAVE OB GAP	A 0.000 D 0.000
WAVE OB HTR	A 0.000 D 0.000
WIND GAP	A 27.31 D 24.01
WIND HTR	A 3.520 D 0.420
WI/WV OG GAP	A 0.000 D 0.000
TX WINDC GAP	A 0.010 D 0.000
TX WINDC HTR	A 0.000 D 0.000
TX TO HEATER	A 0.400 D 0.250
TX TO GAP	A 2.820 D 2.150
STANDBY	A 0.260 D 0.290
IMAGE OG GAP	A 4.080 D 15.15
IMAGE OG HTR	A 0.510 D 2.130
IMAGE OB GAP	A 0.000 D 0.000
TX WVOB GAP	A 0.000 D 0.000
TX WVOB HTR	A 0.000 D 0.000
TX WIND GAP	A 0.080 D 0.410
TX WIND HTR	A 0.040 D 0.020
TX WWOG GAP	A 0.000 D 0.000
TX WWOG HTR	A 0.000 D 0.000
TX WWOB GAP	A 0.640 D 0.380
TX WWOB HTR	A 0.030 D 0.010
NONE	A 7.900 D 3.660
TX TO STBY	A 0.000 D 0.000
TX IMOG GAP	A 0.020 D 0.100
TX IMOG HTR	A 0.010 D 0.030
TX IMOB GAP	A 0.000 D 0.000
TX IMOB HTR	A 0.000 D 0.000
TX WVOG GAP	A 0.000 D 0.000
TX WVOG HTR	A 0.000 D 0.000

ESRIN/PCS   Page 1

FIGURE 8 ERS-2 AMI activity during cycle 138.

4.2 PCS Geophysical Monitoring

The routine analysis is summarized in the plots of figure 9; from top to bottom:

• the monitoring of the valid sigma-nought triplets per day.

• the evolution of the wind direction quality. The ERS wind direction (for all nodes and only for those nodes where the ambiguity removal has worked properly) is compared with the ECMWF forecast. The plot shows the percentage of nodes for which the difference falls in the range -90.0, +90.0 degrees.

• the monitoring of the percentage of nodes whose ambiguity removal works successfully.

• the comparison of the wind speed deviation: (bias and standard deviation) with the ECMWF forecast.

The results since August 6th, 1996 until the beginning of the operation with the Zero Gyro Mode (ZGM) in January 2001 can be summarized as:

• High quality wind products has been distributed since Mid March 1996 (end of calibration and validation phase)

• The number of valid sigma-nought distributed per day was almost stable with a small increase after June 29th, 1999 due to the dissemination in fast delivery of the data acquired in the Prince Albert station (Canada).

• The wind direction is very accurate for roughly 93% of the nodes, the ambiguity removal processing successfully worked for more than 90.0% of the nodes.

• The UWI wind speed shows an absolute bias of roughly 0.5 m/s and a standard deviation that ranges from 2.5 m/s to 3.5 m/s with respect to the ECMWF forecast.

• The wind speed bias and its standard deviation have a seasonal pattern due to the different winds distribution between the winter and summer season.

• Two important changes affect the speed bias plot.

• the first is on June 3rd , 1996 due to the switch from ERS-1 to ERS-2 data assimilation in the meteorological model.

• the second which occurred at the beginning of September 1997, is due to the new monitoring and assimilation scheme in ECMWF algorithms (4D-Var).

• Since 19th April 1999 two set of meteo-table (meteorological forecast centred at 00:00 and 12:00 of each day) are used in the ground processing. This allowed the processing of wind data with 18 and 24 hours meteorological forecast instead of the 18, 24, 30 36 hours forecast. The comparison between data processed with the 18-24 hours forecast instead of 30-36 hours forecast shown an increase in the number of ambiguity removed nodes with a neutral impact in the daily statistics.

• The mono-gyro AOCS configuration (see report for cycle 50) that was operative from 7th February 2000 to 17th January 2001 did not affect the wind data performance.

During the Zero Gyro Mode (ZGM) phase the dissemination of the fast delivery Scatterometer data to the users has been interrupted on 17th January 2001 due to degraded quality in sigma noughts and winds. The satellite attitude in ZGM is slightly degraded and the "old" ground processor was not able to produce calibrated data anymore. For that reason a re-design of the entire ground processing has been carried out and since August 21st 2003 the new processor named ERS Scatterometer Attitude Corrected Algorithm (ESACA) is operative in all the ESA ground station and data was redistributed to the user.

Although for a long period data was not distributed, the PCS has monitored the data quality (as shown in Figure 9) and the results during that period can be summarized as:

At the beginning of the ZGM (January 2001 - end July 2001) the number of valid nodes has clear drop from 190000 per day to 9000 per day. This because the satellite attitude was strong degraded and the received signal had a very high Kp figure (in particular for the far range nodes). For the valid nodes, due to no calibrated sigma nought, the quality of the wind was very poor, the distance from the cone was high and the wind speed bias was above 1.5 m/s.

At the end of July 2001 the ZGM has been tuned and the satellite attitude had an improvement. This explains the increase of the number of valid nodes (returned around the nominal level) and the improvements in the wind speed bias (around 0.5 m/s).

On 4th February 2003, a beta version of the new ESACA processor has been put in operation in Kiruna for validation and the monitoring of the data quality has been done only for the new ESACA data. The number of valid nodes slight decreased because Kiruna station process only 9 of 14 orbits per day. The wind speed direction deviation had a clear improvement because ESACA implements a new ambiguity removal algorithm (MSC) and the ambiguity removal rate is now stable at 100% (the MSC is able to remove ambiguity for all the nodes). The wind speed bias had a clear drop from 0.5 to -0.5 m/s. That value is closer to the nominal one (around -0.2 m/s). As reported in the previous cyclic reports the beta version of ESACA had some calibration problem for the near range nodes and this explains why the data quality does not match exactly the one obtained in the nominal YSM. That problem has been overcome with the final release of the ESACA processor put into operation on August 21st 2003. On June 22nd the failure of the on-board tape recorder discontinued the ERS global mission (see section 4.1) and this explains the low number of valid nodes available after that day.

The performances of ESACA winds delivered between August 2003 and September 2004 are affected by land contamination. Around costal zones many Sea nodes have a strong contribution of Land backscattering and the retrieved wind is not correct. An optimization of

the Land/Sea flag in the ground processing has been carried out during the cycle 98. In the statistics computed by PCS on the fast delivered winds the Land contamination has been removed by using a refined Land/Sea mask. Also the ice contamination has been removed with a simple geographical filter. With these new setting the PCS statistics are very similar to the ones reported by ECMWF.

For cycle 138 the wind performances stayed stable. The wind speed bias (UWI vs 18 or 24 hour forecast) was roughly 0.9 m/s and the speed bias standard deviation was around 1.6 m/s.

The reduced number of nodes available on 30th June is due to a problem in the Esrin dissemination facility.

The wind direction deviation for cycle 138 was good with more than 98% of the nodes wind direction in agreement with the ECMWF forecast.
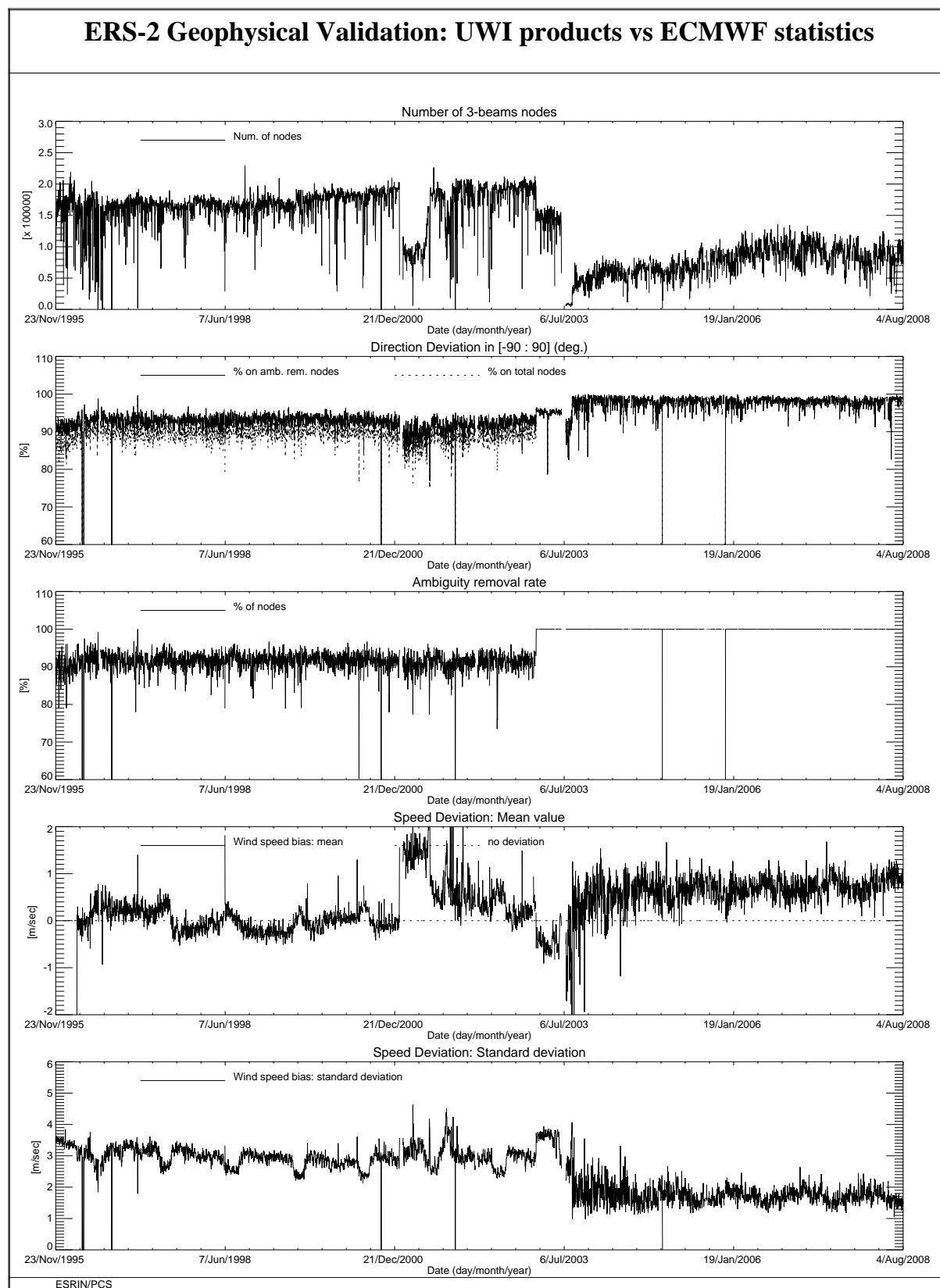
FIGURE 9 ERS-2 Scatterometer: wind products performance since the beginning of the mission.
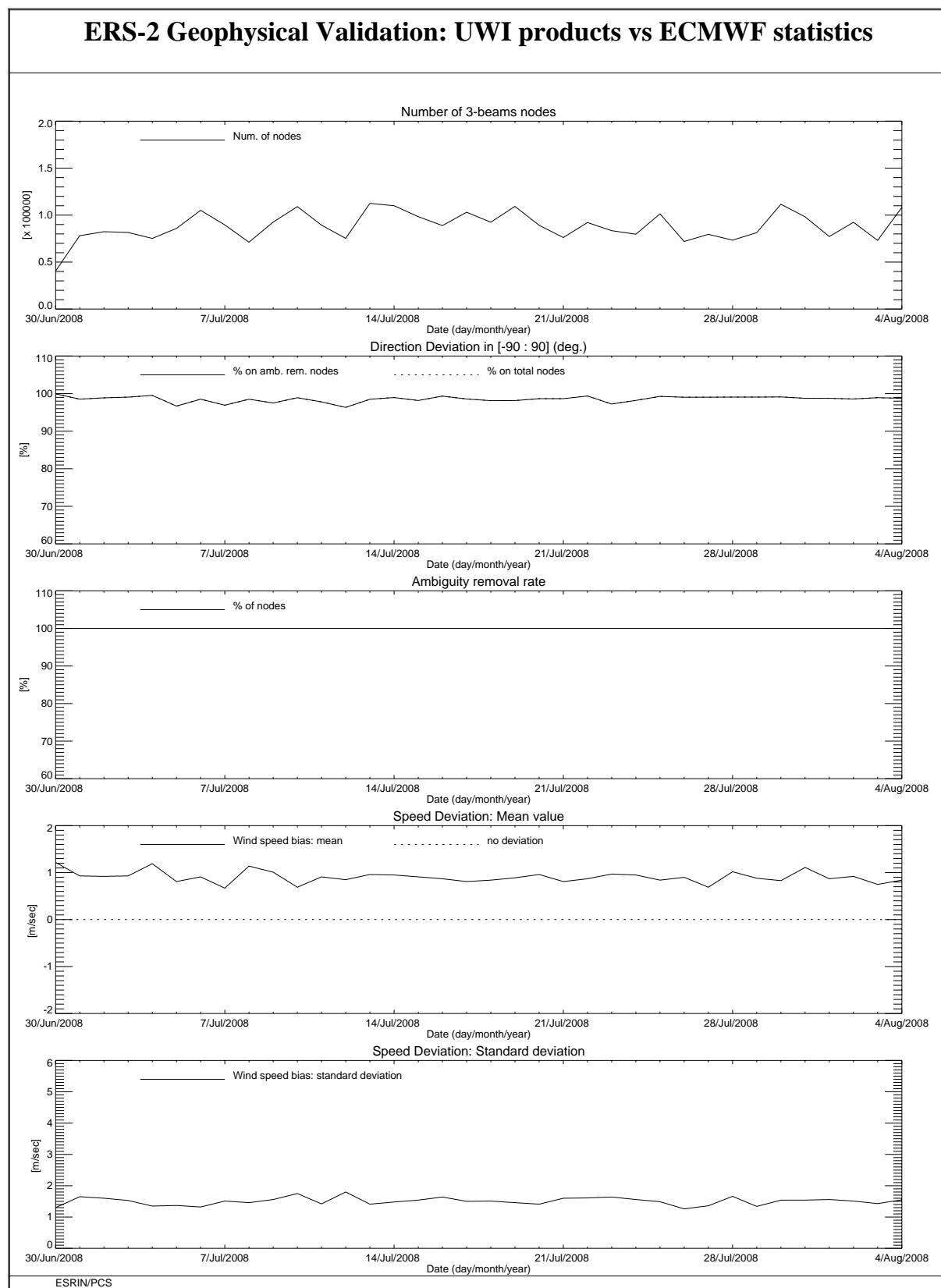
FIGURE 10 ERS-2 Scatterometer: wind products performance for cycle 138.

4.3 ECMWF Geophysical Monitoring

The quality of the UWI product was monitored at ECMWF for Cycle 138. Results were compared to those obtained from the previous Cycle, as well for data received during the nominal period in 2000 (up to Cycle 59). No corrections for duplicate observations were applied.

During Cycle 138 data was received between 21:15 UTC 30 June 2008 and 20:27 UTC 4 August 2008. Data was grouped into 6-hourly batches (centred around 00, 06, 12 and 18 UTC). Data was received for all batches.

Data is being recorder whenever within the visibility range of a ground station. For Cycle 138, data coverage was over the North-Atlantic, the Mediterranean, the Gulf of Mexico, a small part of the Pacific west from the US, Canada and Central America, a small part of the Atlantic and Indian Ocean around South Africa, the Chinese Sea, a small part of the Indian Ocean South-East of Thailand and Indonesia, and the Southern Ocean close to the Antarctic and south of Australia and New Zealand.

The asymmetry between the fore and aft incidence angles did not show large peaks. Solar activity was low during Cycle 138 (source www.spaceweather.com).

Compared to Cycle 137, the UWI wind speed relative to ECMWF first-guess (FG) fields showed a lower standard deviation (1.29 m/s, was 1.31 m/s). Bias levels were similar as well (on average -1.11 m/s, was -1.10 m/s).

The ECMWF operational assimilation and forecast system was not changed during Cycle 138.

The Cycle-averaged evolution of performance relative to ECMWF first-guess (FG) winds is displayed in Figure 11. Figure 12 shows global maps of the over Cycle 138 averaged UWI data coverage and wind climate, Figure 13 for performance relative to FG winds.
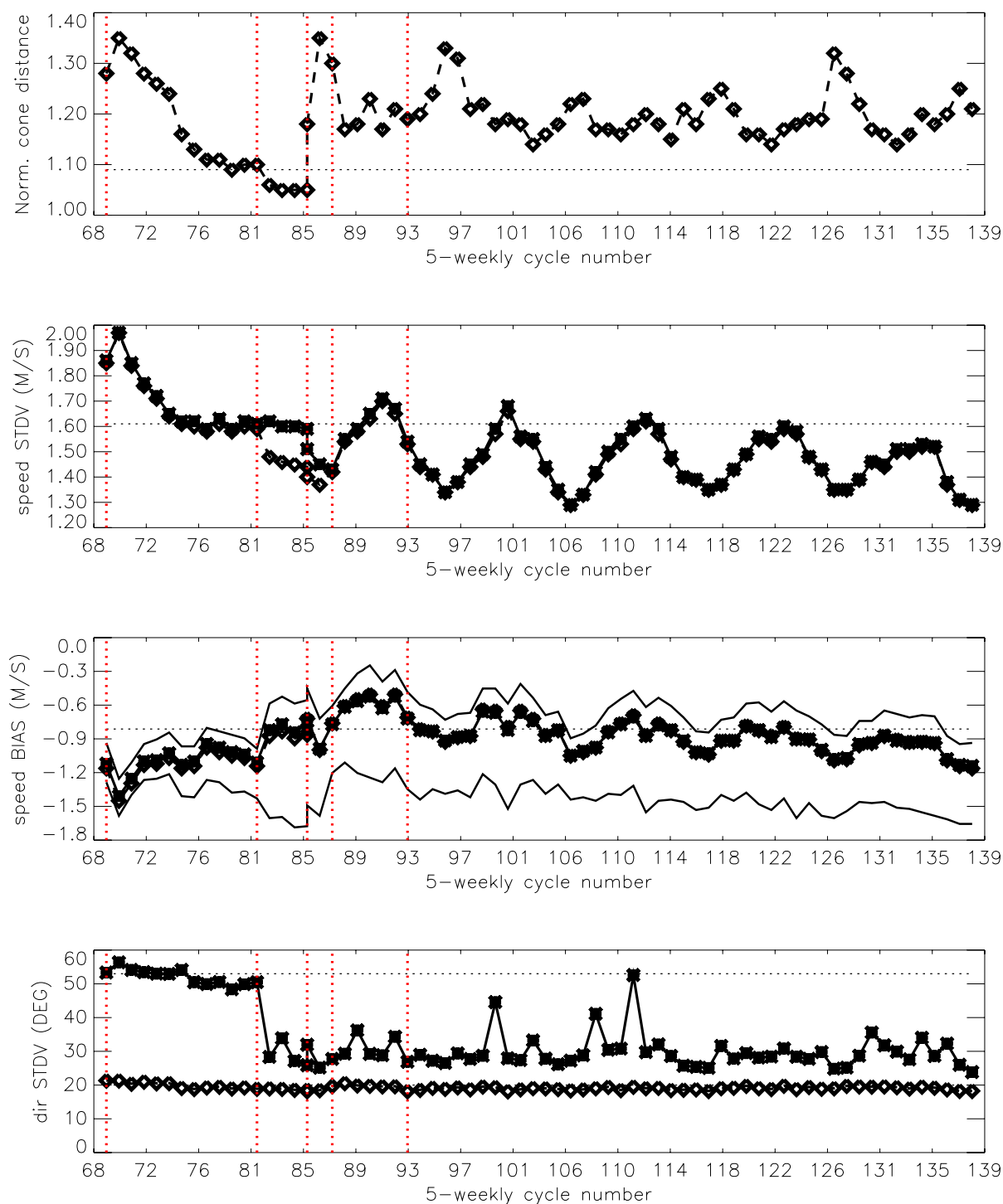
FIGURE 11 Evolution of the performance of the ERS-2 Scatterometer averaged over 5-weekly cycles from 12 December 2001 (cycle 69) to 4 August 2008 (end cycle 138) for the UWI product (solid, star) and de-aliased winds based on CMOD4 (dashed, diamond). Results are based on data that passed the UWI QC flags. For cycle 85 two values are plotted; the first value for the global set, the second one for the regional set. Dotted lines represent values for cycle 59 (5 December 2000 to 17 January 2001),i.e. the last stable cycle of the nominal period. From top to bottom panel are shown the normalized distance to the one (CMOD4 only) the standard deviation of the wind speed compared to FG winds, the corresponding bias (for UWI winds the extreme inter-node averages are shown as well), and the standard deviation of wind direction compared to FG.

NOBS (ERS-2 UWI), per 12H, per 125km box
average from 200807010O to 20080804l8 GLOB:2.29

FIGURE 12 Average number of observations per 12H and per 125km grid box (top panel) and wind-climate (lower panel) for UWI winds that passed the UWI flags QC and a check on the collocated ECMWF land and sea-ice mask.

BIAS (ERS-2 UWI vs FIRST-GUESS), in m/s.
average from 2008070100 to 2008080418 GLOB:-1.03
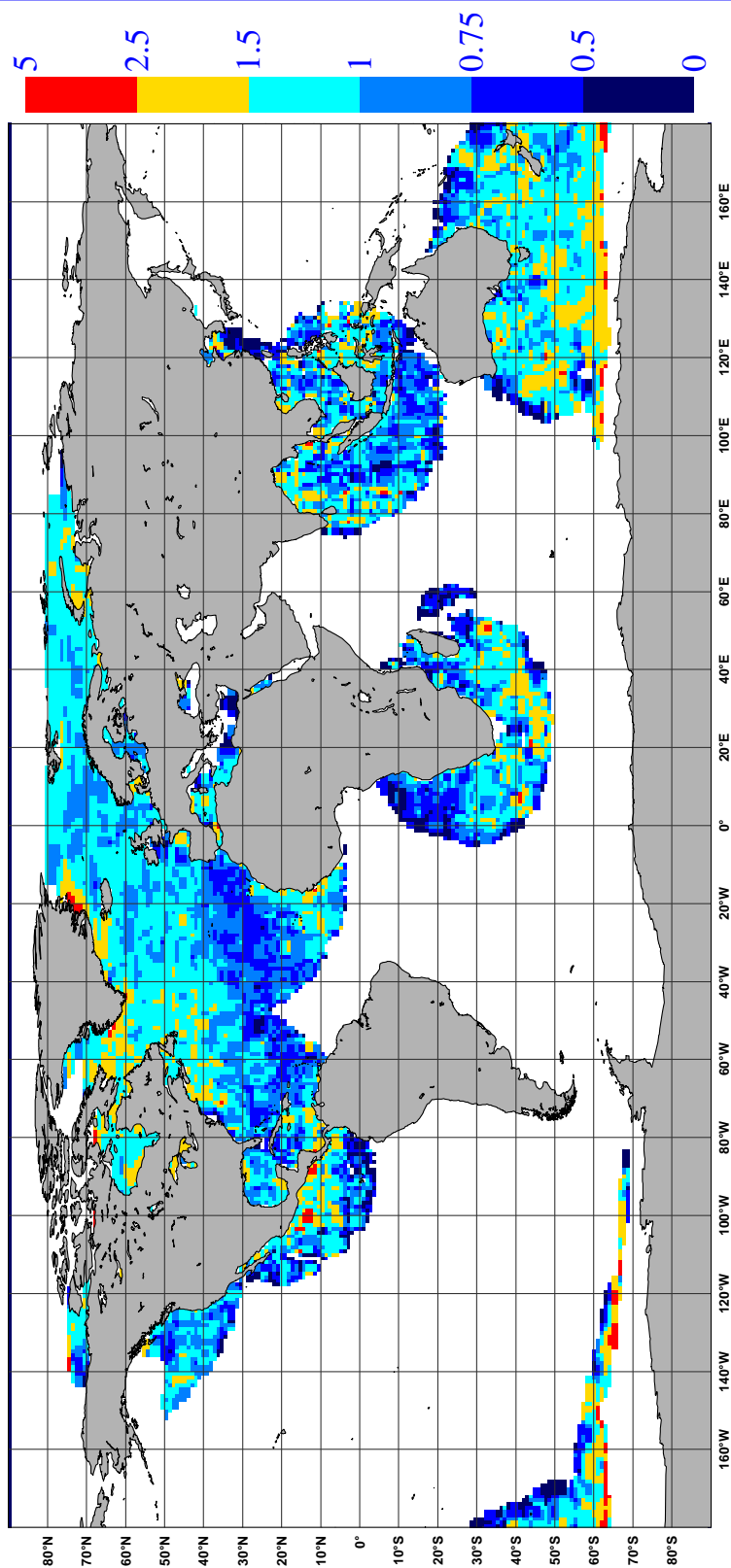
FIGURE 13 The same as Figure 12, but now for the relative bias (top panel) and standard deviation (lower panel) with ECMWF first-guess winds.

4.3.1 Distance to cone history

The distance to the cone history is shown in Figure 14. Curves are based on data that passed all QC, including the test on the K_p-yaw flag, and subject to the land and sea-ice check at ECMWF (see cyclic report 88 for details).

Like for previous cycles, time series are (due to lack of statistics) very noisy, especially for the near-range nodes. Most spikes were found to be the result of low data volumes.

Compared to cycle 137, the average level was somewhat lower (1.21 versus 1.25), which is higher (by 11%) than for nominal data (see top panel Figure 11).

The fraction of data that did not pass QC is displayed in Figure 14 as well (dash curves).
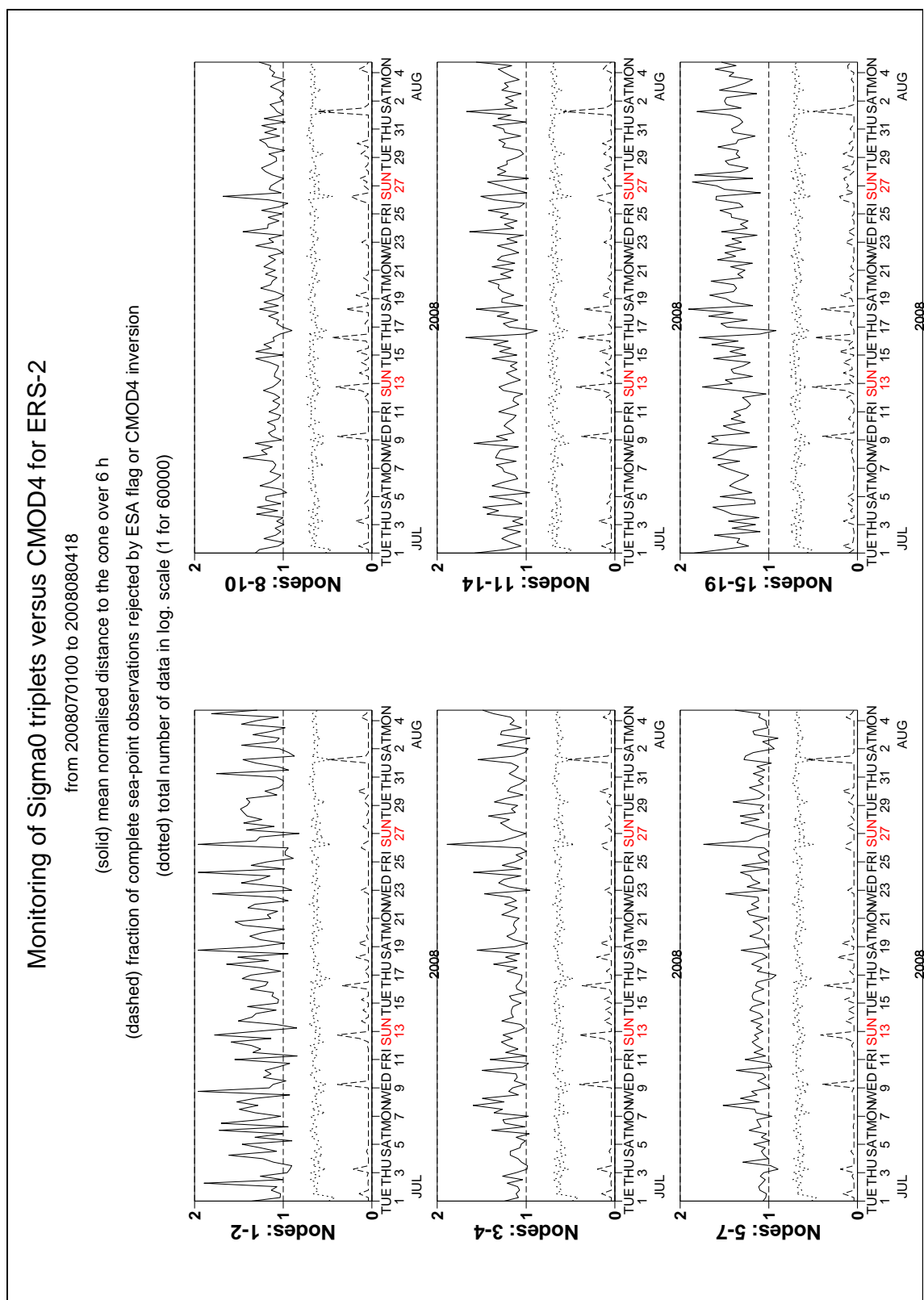
FIGURE 14 Mean normalized distance to the cone computed every 6 hours for nodes 1-2, 3-4, 5-7, 8-10, 11-14 and 15-19 (solid curve close to 1 when no instrumental problems are present). The dotted curve shows the number of incoming triplets in logarithmic scale (1 corresponds to 60,000 triplets) and the dashed one indicates the fraction of complete (based on the land and sea-ice mask at ECMWF) sea-located triplets rejected by ESA flags, or by the wind inversion algorithm (0: all data kept, 1: no data kept).

4.3.2 UWI minus First-Guess history

In Figure 15, the UWI minus ECMWF first-guess wind-speed history is plotted. The history plot shows a few peaks, which are usually the result of low data volume.

Figure 19 displays the locations for which UWI winds were more than 8 m/s weaker (top panel), respectively more than 8 m/s stronger (lower panel) than FG winds. Like for cycle 137, such collocations are isolated, and often indicate meteorologically active regions, for which UWI data and ECMWF model field show reasonably small differences in phase and/or intensity.
Deviations near the poles are the result of imperfect sea-ice flagging.

Two cases for which UWI winds were considerably different from FG winds are presented in Figure 20. The case in the top panel (12 July 2008 south of Mexico) shows the capture of Hurricane Elida at an early stage of its development (tropical storm at the time).
UWI winds give a much stronger and slightly shifted circulation compared to the ECMWF FG wind field. The scatterometer winds suffer from de-aliasing problems, though. ASCAT captured the same area in a consistent way, and the usage of both instruments in the ECMWF analysis moved the vortex westwards (not shown). The lower panel shows a case of a degraded patch of UWI winds on 21 July 2008, also south of Mexico.

Average bias levels and standard deviations of UWI winds relative to FG winds are displayed in Table 6. From this it follows that the bias of UWI winds was more negative (-1.11 m/s, was -1.10 m/s), being around -0.3 m/s more negative than the nominal data in 2000.

Table 6 Wind speed and direction biases

	Cycle 137		Cycle 138	
	UWI	CMOD4	UWI	CMOD4
Speed STDV	1.38	1.37	1.31	1.31
Node 1-2	1.42	1.40	1.38	1.37
Node 3-4	1.36	1.35	1.32	1.31
Node 5-7	1.32	1.32	1.27	1.27
Node 8-10	1.34	1.34	1.25	1.25
Node 11-14	1.34	1.34	1.27	1.27
Node 15-19	1.36	1.36	1.30	1.30
Speed BIAS	-1.05	-1.06	-1.10	-1.11
Node 1-2	-1.57	-1.55	-1.61	-1.59
Node 3-4	-1.32	-1.29	-1.34	-1.31
Node 5-7	-1.08	-1.07	-1.10	-1.09
Node 8-10	-0.90	-0.90	-0.95	-0.96
Node 11-14	-0.85	-0.87	-0.92	-0.95
Node 15-19	-0.87	-0.92	-0.94	-0.99
Direction STDV	32.3	18.7	26.0	18.3
Direction BIAS	-1.1	-1.3	-0.8	-1.2

On a longer time scale seasonal bias trends are observed (see Figure 11). As was highlighted in the previous cyclic reports, it is believed that this yearly trend is partly induced by changing local geophysical conditions. Strong indication for this is a similar trend observed for QuikSCAT data when restricted to an area well-covered by ERS-2 (20N-90N, 80W-20E).

Figure 25 shows time series for that area for both ERS-2 (top panel) and QuikSCAT (lower panel) for the period between 1 January 2004 and 4 August 2008 (end of cycle 138). Results are displayed for at ECMWF actively assimilated data, i.e., CMOD5 winds for ERS-2 and 4%-reduced QuikSCAT winds on a 50km resolution. The quick development of a negative bias for both ERS-2 and QuickSCAT data during the last Cycle is also observed for previous years.

Note the increase in ERS-2 wind speed as used at ECMWF since the introduction of the new model cycle at ECMWF on 7 June 2007. It reflects a switch at ECMWF from the CMOD5 to CMOD5.4 model function, which has enhanced the Scatterometer wind speed by 0.48 m/s.

The standard deviation of UWI wind speed versus ECMWF FG was, compared to cycle 137,

slightly lower (1.29 m/s, was 1.31 m/s).

For cycle 138 the (UWI - FG) direction standard deviations were mostly ranging between 20 and 40 degrees (Figure 17) representing nominal variations. Compared to Cycle 137 average STDV for UWI wind direction has improved (23.80 degrees, was 26 degrees). For at ECMWF de-aliased winds performance was stable (STDV 18.3 degrees, unchanged).
Degradation in wind direction on 17th July is due to meteo tables not ingested in the processing due to an Esrin ground segment dissemination problem.
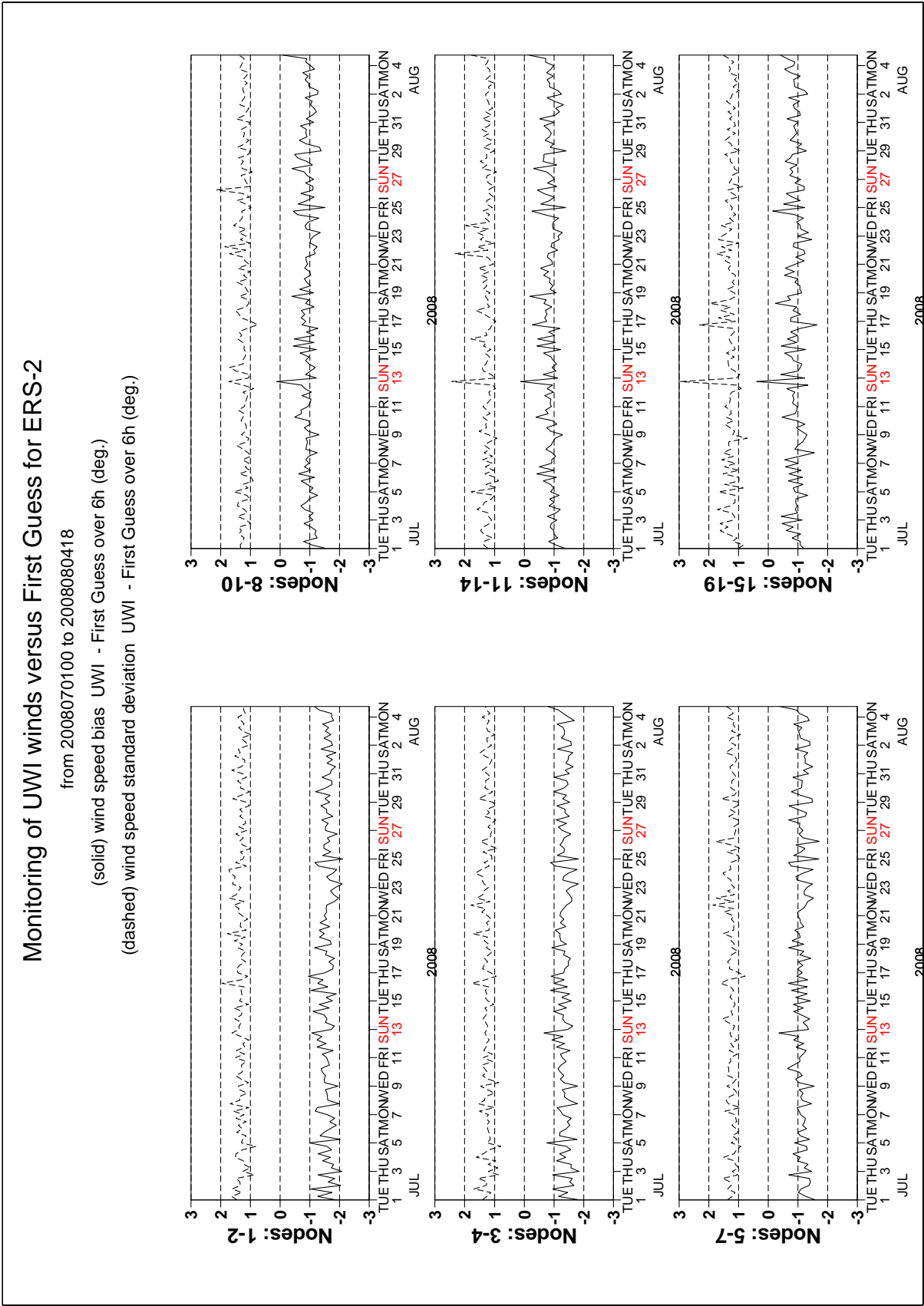
FIGURE 15 Mean (solid line) and standard deviation (dashed line) of the wind speed difference UWI - first guess for the data retained by the quality control.
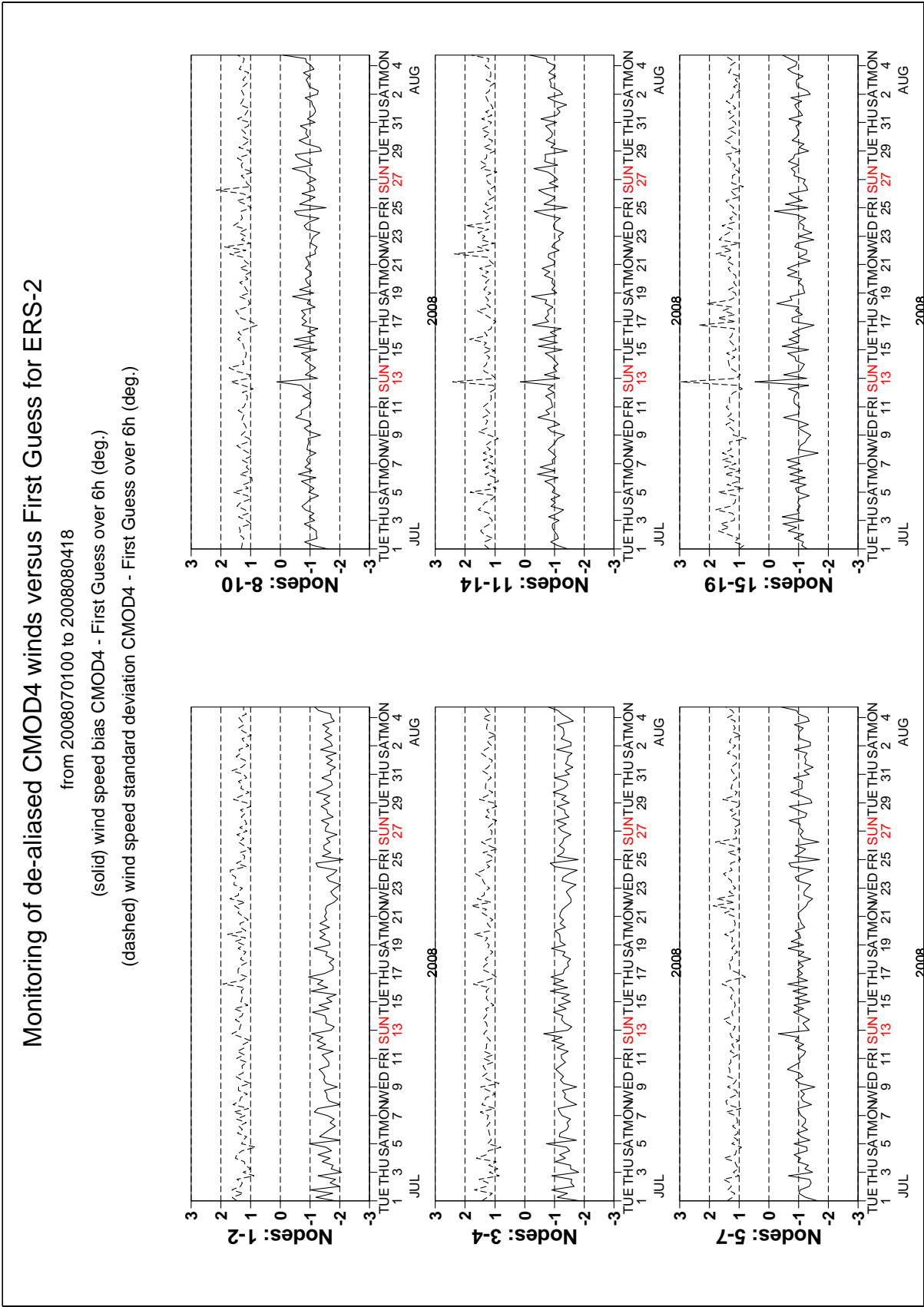
FIGURE 16 Same as Fig. 15, but for the de-aliased CMOD4 data.

FIGURE 17 Same as Fig. 15, but for the wind direction difference. Statistics are computed only for wind speeds higher than 4 m/s.
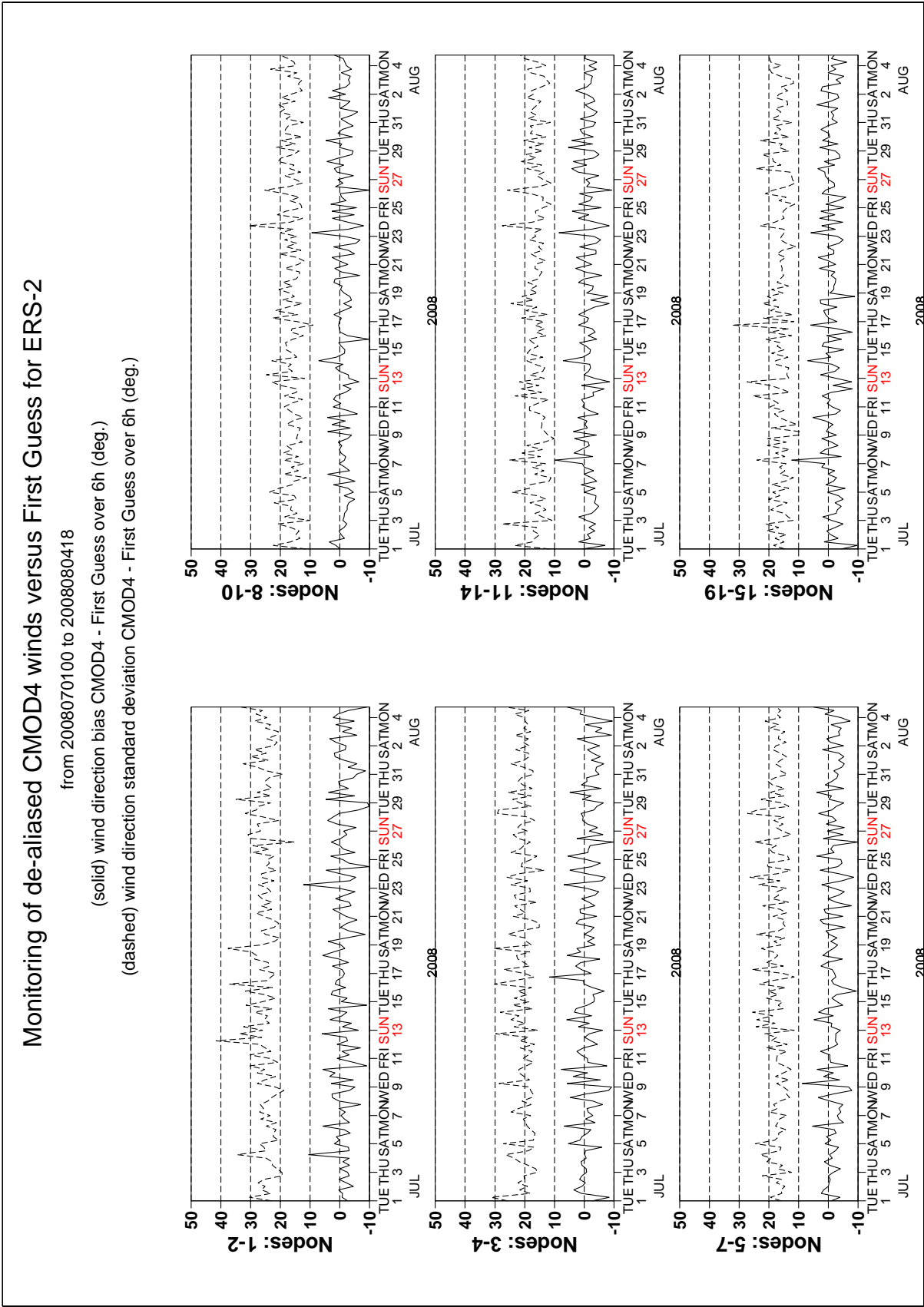
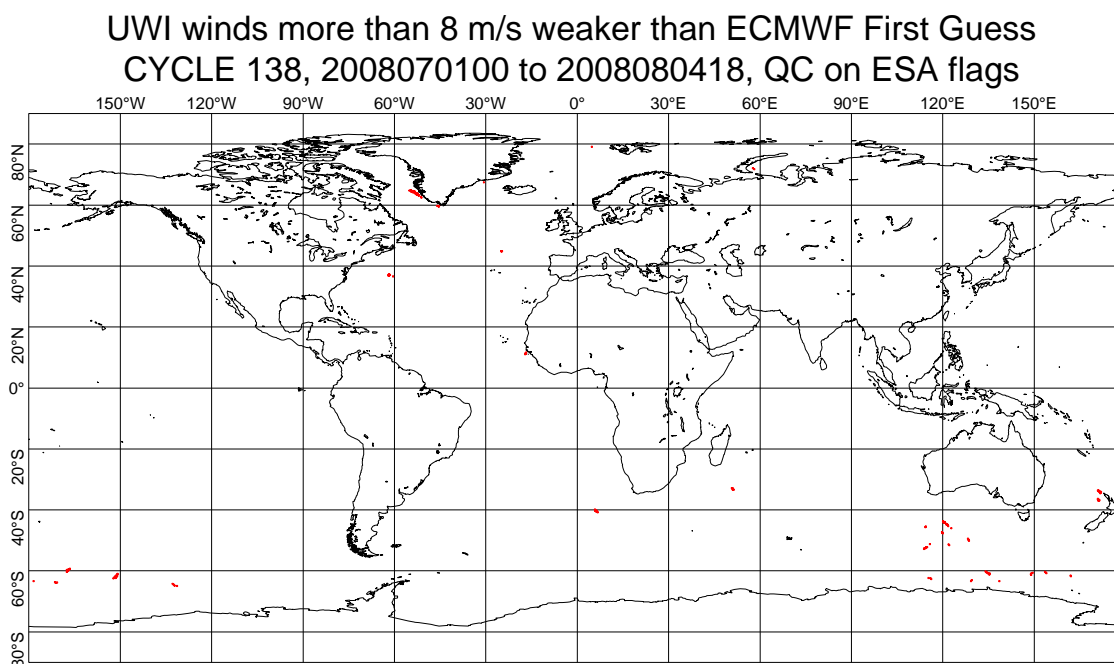**FIGURE 18 Same as Fig. 17, but for the de-aliased CMOD4 data.**

UWI winds more than 8 m/s weaker than ECMWF First Guess
CYCLE 138, 2008070100 to 2008080418, QC on ESA flags

UWI winds more than 8 m/s stronger than ECMWF First Guess
CYCLE 138, 2008070100 to 2008080418, QC on ESA flags
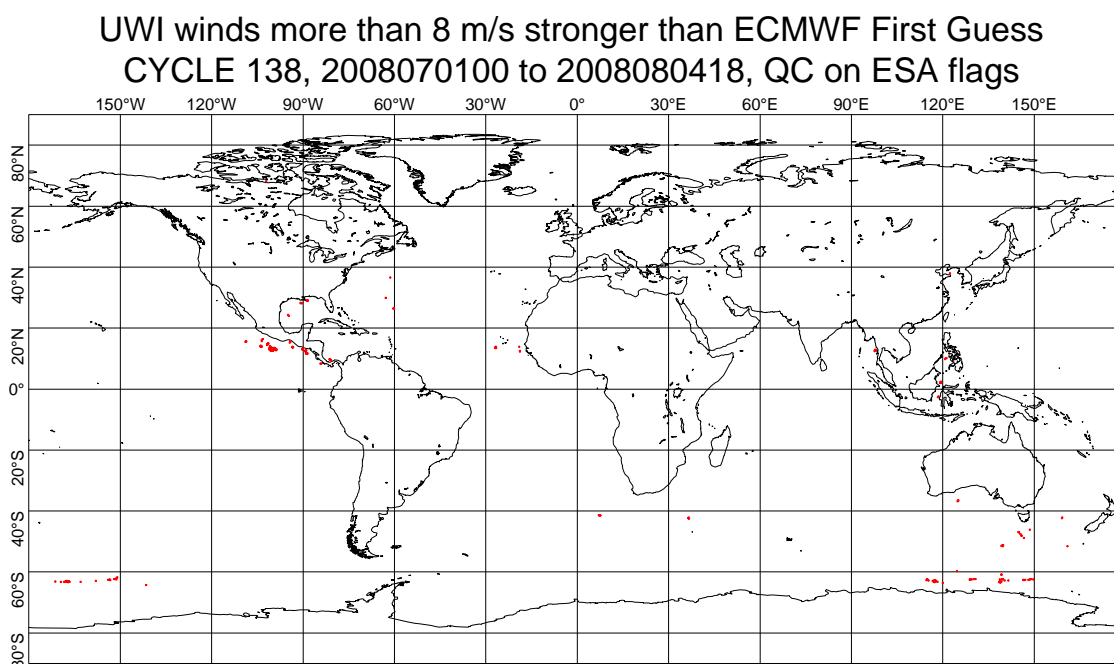
FIGURE 19 Locations of data during cycle 138 for which UWI winds are more than 8 m/s weaker (top panel) respectively stronger (lower panel) than FGAT, and on which QC on UWI flags and the ECMWF land/sea-ice mask was applied.
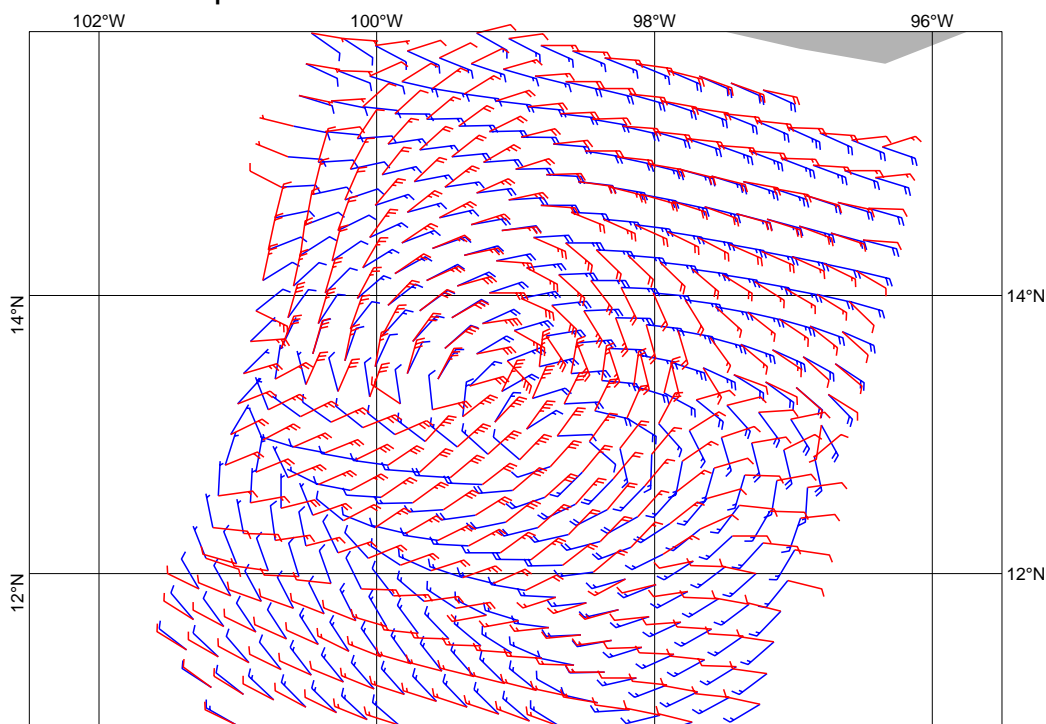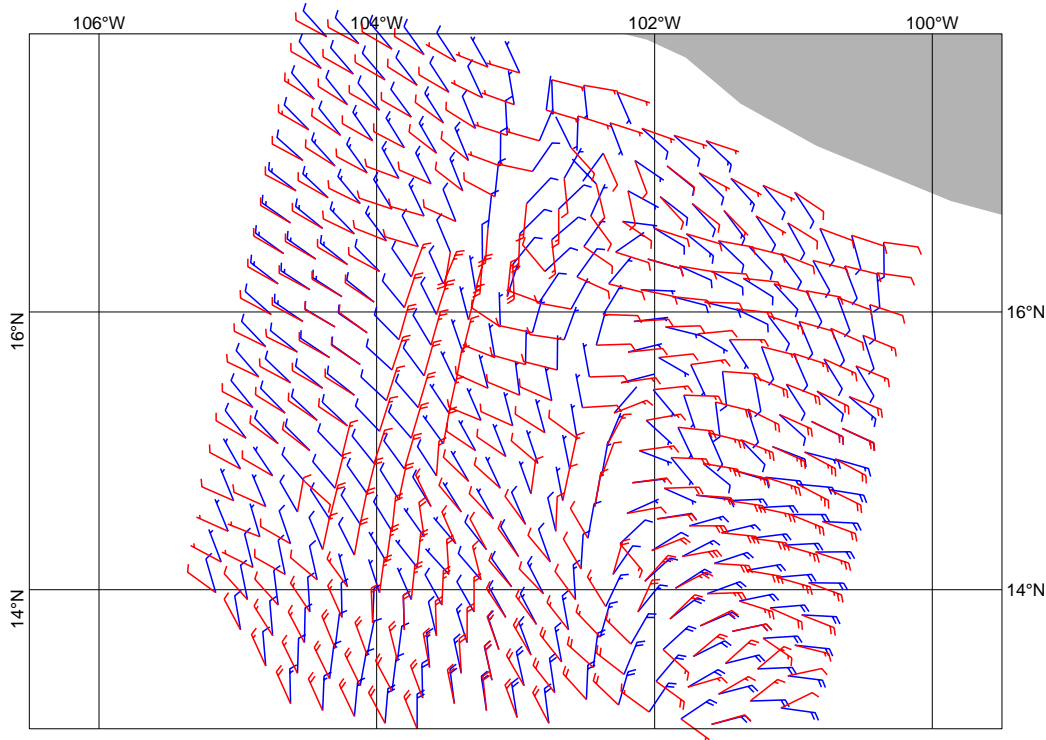
FIGURE 20 Comparison between UWI winds (in red) and ECMWF FG winds (in blue) for hurricane Elida on 12 July 2008 (top panel) and for a case on 21 July 2008 (lower panel), both captured south of Mexico.

4.3.3 Scatter plots

Scatter plots of FG winds versus ERS-2 winds are displayed in Figures 21 to 24. Values of standard deviations and biases are slightly different from those displayed in Table 6. Reason for this is that, for plotting purposes, the in 0.5 m/s resolution ERS-2 winds have been slightly perturbed (increases scatter with 0.02 m/s), and that zero wind-speed ERS-2 winds have been excluded (decreases scatter with about 0.05 m/s).

The scatter plot of UWI wind speed versus FG (Figure 21) is very similar to that for (at ECMWF inverted) de-aliased CMOD4 winds (Figure 23). It confirms that the ESACA inversion scheme is working properly.

Winds derived on the basis of CMOD5 are displayed in Figure 24. The relative standard deviation is lower than for CMOD4 winds (1.27 m/s versus 1.32 m/s). Compared to ECMWF FG, CMOD5 winds are 0.66 m/s slower.
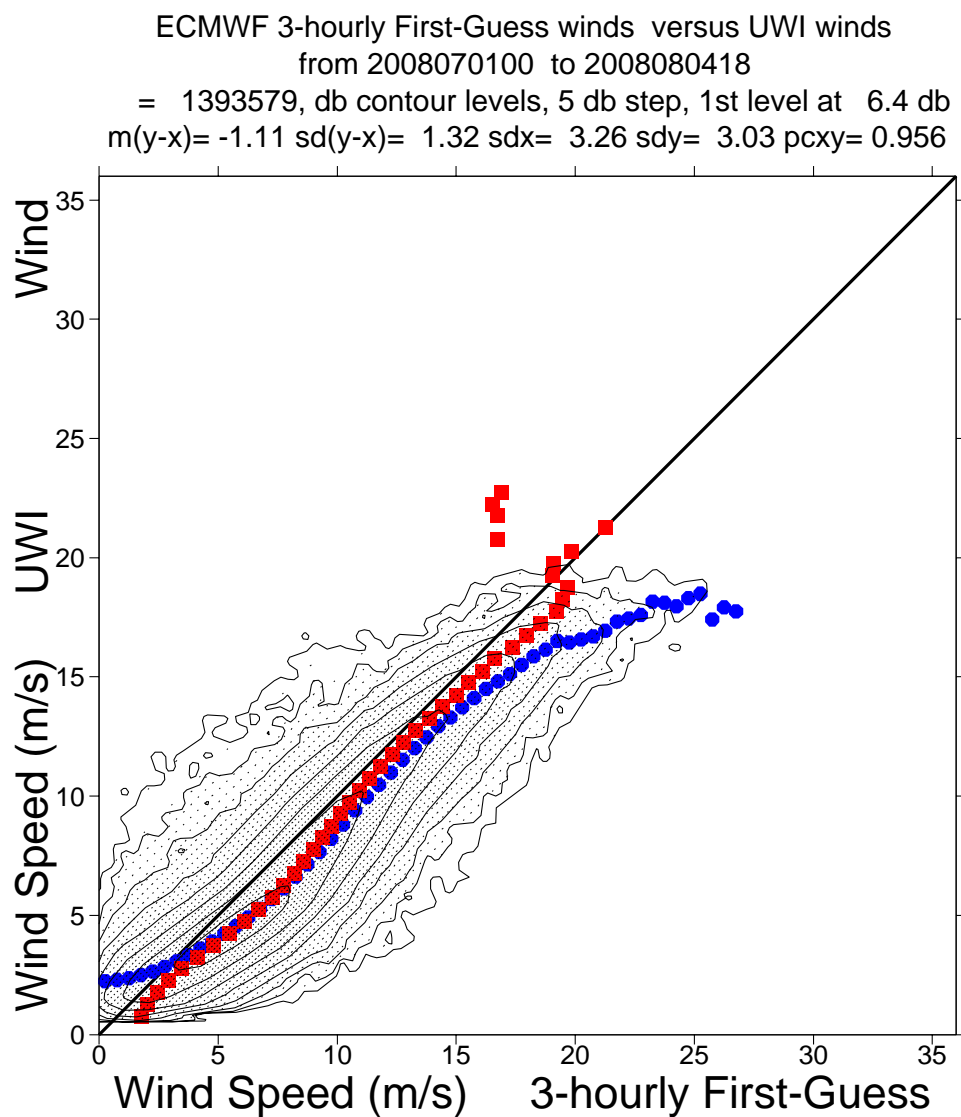
FIGURE 21 Two-dimensional histogram of first guess and UWI wind speeds, for the data kept by the UWI flags, and QC based on the ECMWF ice and land and sea-ice mask. Circles denote the mean values in the y-direction and squares those in the x-direction.
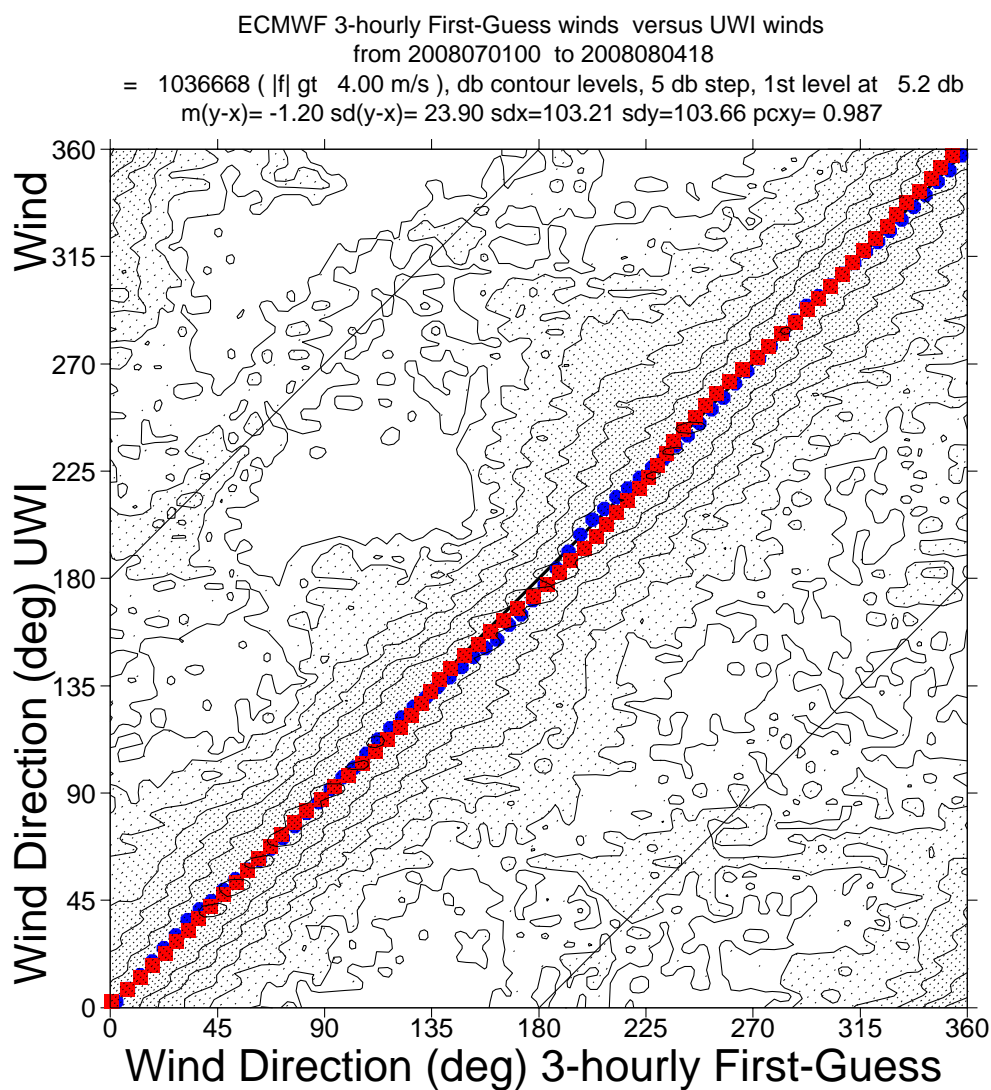
ECMWF 3-hourly First-Guess winds versus UWI winds
from 2008070100 to 2008080418
= 1036668 (|f| gt 4.00 m/s), db contour levels, 5 db step, 1st level at 5.2 db
m(y-x)= -1.20 sd(y-x)= 23.90 sdx=103.21 sdy=103.66 pcxy= 0.987

FIGURE 22 Same as Fig. 21, but for wind direction. Only wind speeds higher than 4m/s are taken into account.

ECMWF 3-hourly First-Guess winds versus CMOD4 winds
from 2008070100 to 2008080418
= 1367546, db contour levels, 5 db step, 1st level at   6.4 db
m(y-x)= -1.12 sd(y-x)= 1.32 sdx= 3.22 sdy= 3.00 pcxy= 0.955
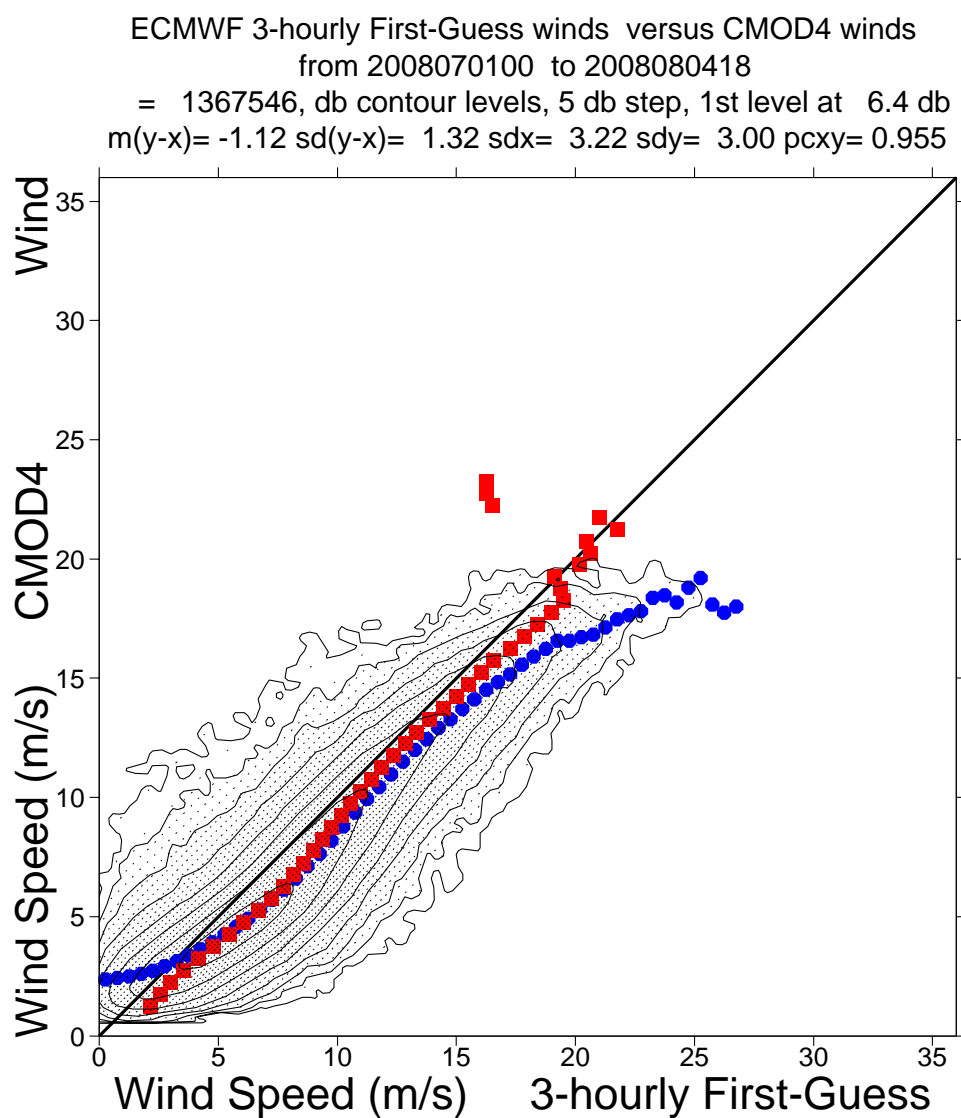
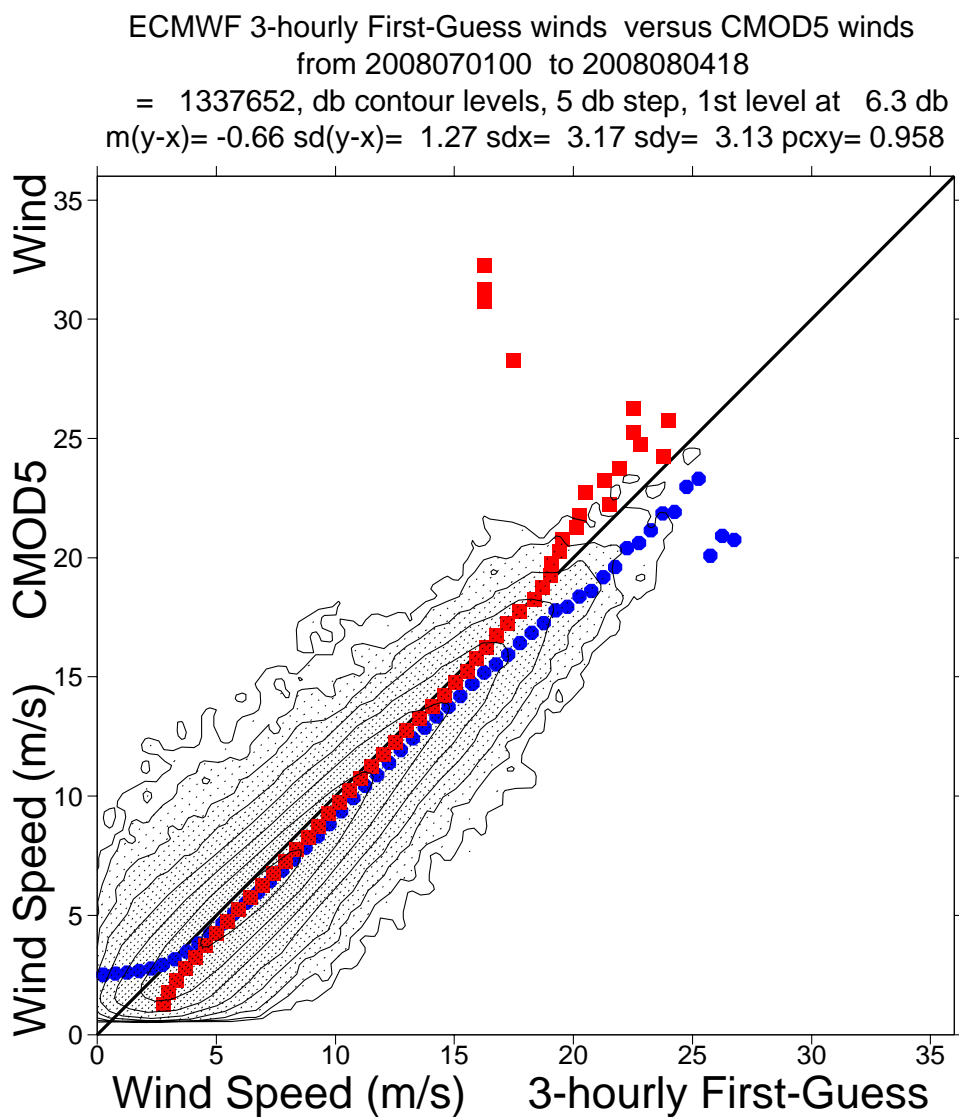**FIGURE 23 Same as Fig. 21, but for de-aliased CMOD4 winds.**

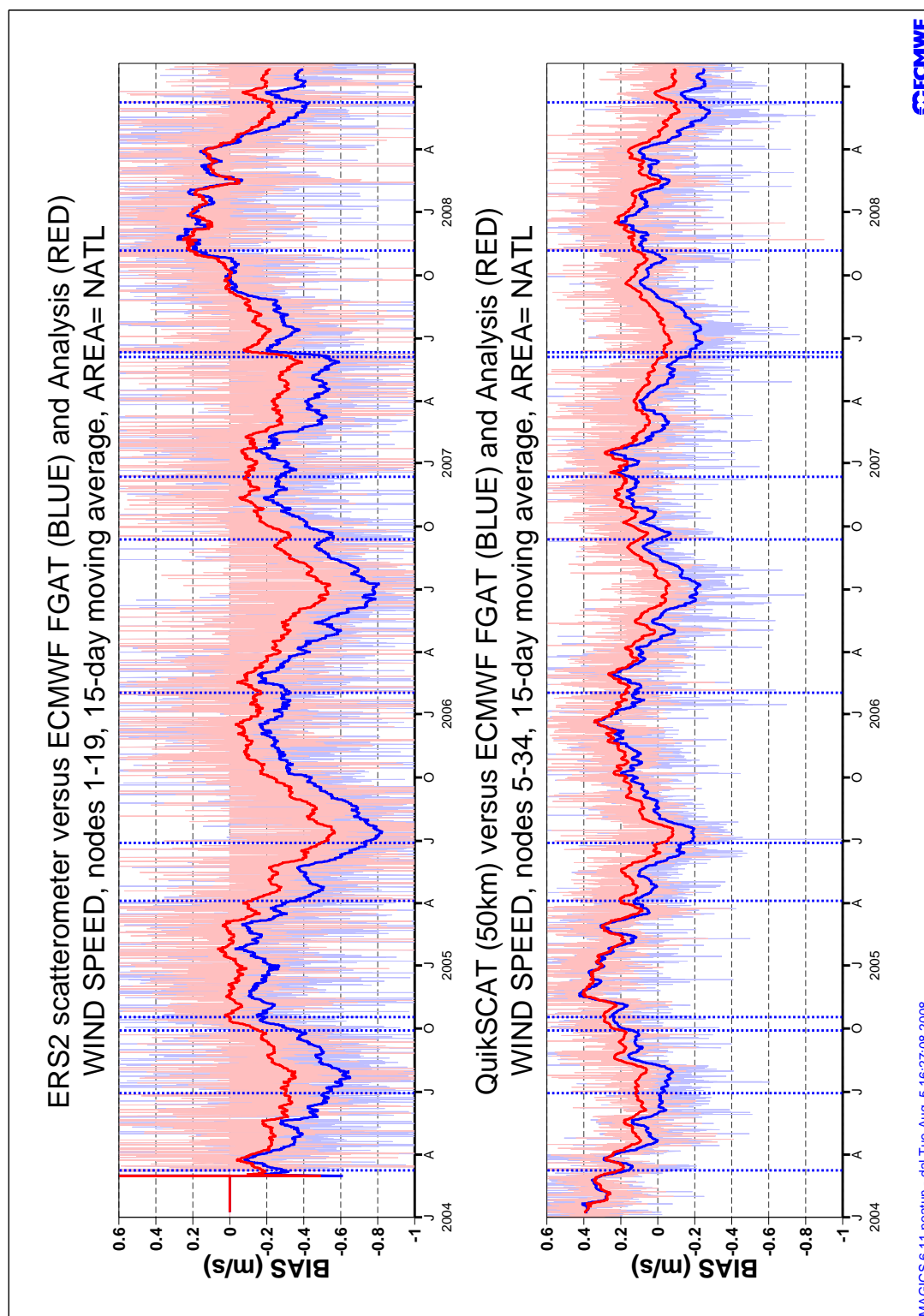**FIGURE 24 Same as Fig. 21, but for de-aliased CMOD5 winds.**

FIGURE 25 Bias relative to FG winds for actively assimilated ERS-2 winds (based on CMOD5) for nodes 1-19 (top panel) respectively of 50-km QuikSCAT (based on the QSCAT-1 model function and reduced by 4%) for nodes 5-34 (lower panels) averaged over the area (20N-90N, 80W-20E), and displayed for the period 01 January 2004 – 4 August 2008. Fat curves represent centered 15-day running means, thin curves values for 6-hourly period. Vertical dashed blue lines mark ECMWF model changes

4.3.4 Timeliness evolution

The Scatterometer product timeliness is defined as the difference between the acquisition time of the first product and the creation date of the file received in ESRIN-PCS. Once the UWI file is received in ESRIN, data are converted in BUFR format and sent to users via the GTS network. Therefore that timeliness is an indicator of the delay time that the user could expect in the data dissemination. The analysis does not take into account delays in the GTS network. For each file received from the ground station, the timeliness is computed and this analysis reports the daily mean timelines obtained by averaging all the values.

The analysis has been performed on the daily timeliness average. Timeliness is zero when no products are received.

In the next figures is showed the evolution of the daily mean timeliness of Kiruna, Maspalomas, Gatineau, West Freugh and Miami stations since April 2005. Since 2007 the analysis has been extended also first to McMurdo and Beijing products and then to Matera, Hobart, Singapore and Chetumal products. The starting date of the analysis, for each station, is reported in the following table:

TABLE 6 Starting date of Timeliness analysis for each station

STATION	START DATE
Kiruna	19 April 2005
Gatineau	19 April 2005
Maspalomas	19 April 2005
West Freugh	19 April 2005
Miami	19 April 2005
McMurdo	13 March 2007
Beijing	13 March 2007
Matera	5 December 2007
Hobart	5 December 2007
Singapore	5 December 2007
Chetumal	5 December 2007
Johannesburg	17 July 2008

The Figure 26 shows the results of the investigation for Gatineau, Kiruna, Maspalomas, Matera and Singapore stations.
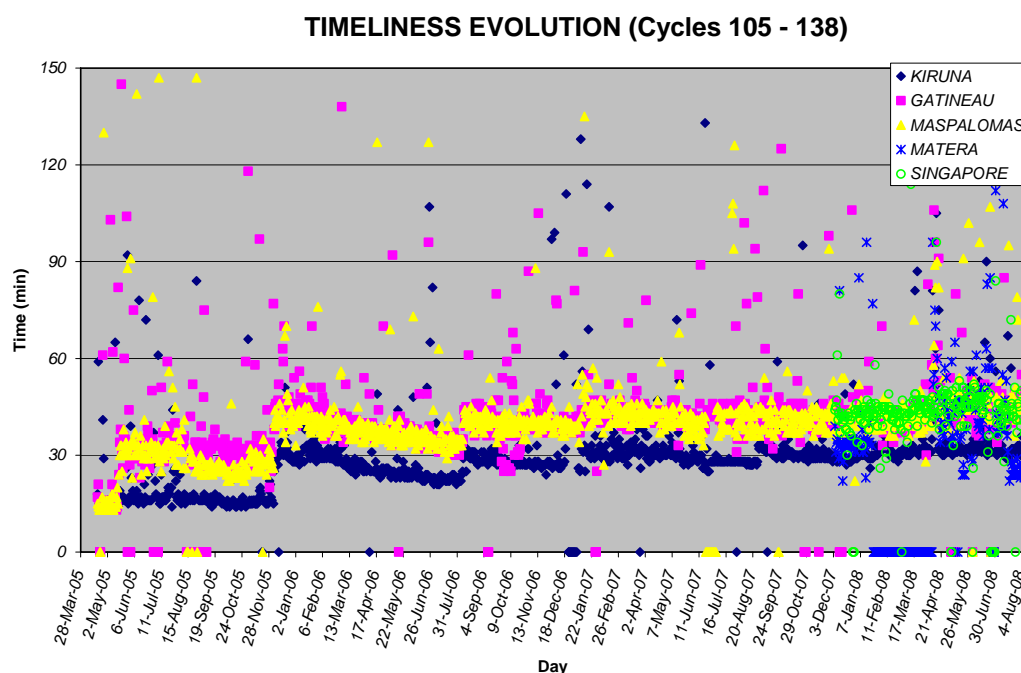
FIGURE 26 Timeliness evolution from 19th April 2005 to 4th August 2008 for Gatineau, Kiruna, Maspalomas, Matera and Singapore ground stations.

Apart from some values out of the general tendency due to temporary system or connection problem, since the beginning of the analyzed period a timeliness increase is detected for Kiruna, Maspalomas and Gatineau stations. In particular, it can be recognized a discontinuous trend for the three stations with quickly increases in the same days for the 3 stations followed by a slightly decrease in the subsequent months. In depth analysis showed that these rapid increases occur about in the following days: 5 May 2005, 5 December 2005, 9 August 2006 and 9 January 2007. This behavior could be due to settings modifications in the ground segment.

During the cycles 138 Gatineau, Maspalomas and Singapore remain stable with a timeliness value of 45 minutes. A slight decrease of the timeliness can be observed for Matera station that reached a value of about 25 minutes, the lowest timeliness in the reporting period. Kiruna is stable around 30 minutes.

The analysis for West Freugh, Miami, Beijing, McMurdo, Hobart, Chetumal and Johannesburg stations is showed in Figure 27.
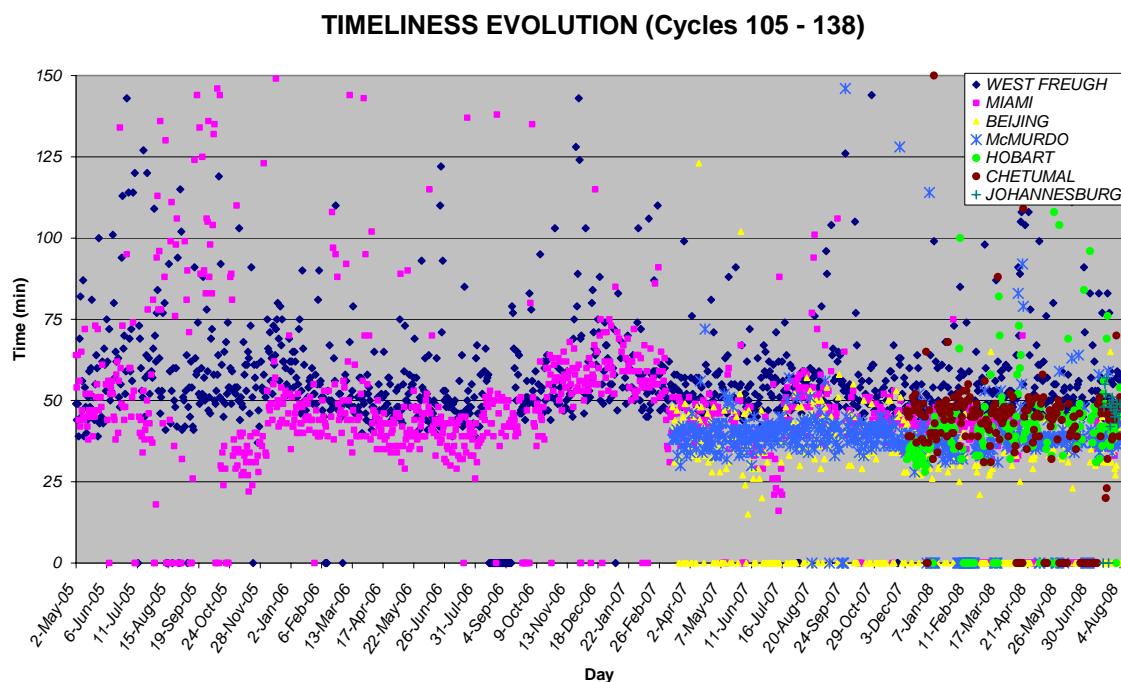
FIGURE 27 : Timeliness evolution from 19 April 2005 to 4th August 2008 for West Freugh, Miami, Beijing, McMurdo, Hobart, Chetumal and Johannesburg ground stations.

West Freugh and Miami stations show a similar regular trend in the analyzed period. More in detail a slightly increased timeliness could be identified since October 2006 followed by a decrease since January 2007. Nowadays West Freugh products have an average timeliness of 50 minutes, Miami around 45 minutes.

The analysis for McMurdo and Hobart stations shows a lower timeliness that is around 40 minutes for all the stations. Beijing has the lowest timeliness with values around 30 minutes. The last ground stations, Chetumal and Johannesburg have instead a high timeliness of about 50 minutes.

The analysis carried out shows that till December 5th 2005 UWI products delivered from the three ESA ground station (Kiruna, Maspalomas, Gatineau) had a timeliness that fulfils the requirements for nowcasting application (data received on average within 25 minutes). After that date performances degraded and nowadays the average timeliness is around 35 minutes. This trend needs further investigations to better understand the cause.

5   Yaw error angle estimation

The yaw error angle estimation is computed on-ground by the ESACA processors. The full set of results of the yaw processing is stored in an internal ESA product named HEY (Helpful ESA Yaw) disseminated from the ground station to ESRIN. The estimation of the yaw error angle is based on the Doppler shift measured on the received echo. That estimation can be done with a good accuracy only for small yaw error angle (in the range between +/-4 deg.). Above that range, due to high Doppler frequency shift the signal spectrum is outside the receiver bandwidth and the yaw estimation is strong degraded. Details regarding the yaw processing can be found on the following document (chapter 9): http://earth.esa.int/pcs/ers/scatt/articles/soamain-030521.pdf .

The yaw error angle estimation aims to compute the correct acquisition geometry for the three Scatterometer antenna throughout the entire orbit. The Yaw error angle information is used in the radar equation to derive the calibrated backscattering (sigma nought) from the Earth surface and to select the echo samples associated to one node. In ESACA the definition of the node position is as the one adopted in the old processor (for details see:.http://earth.esa.int/pcs/ers/scatt/articles/scatt_work98_processing.pdf). In such way the distance between the nodes (both along and across track) is kept constant (25 Km) and what is changing in function of the yaw error angle is the number of echo samples that contributes to the node calculation and the incidence angle of the measurement. This because the three Scatterometer antennae could see the node with a different geometry due to an arbitrary variation of the yaw angle along track. The number of samples that actually contributes to a node and the yaw flag can be retrieved from the UWI Data Set Record (DSR) product. For that reason the definition of few fields in the UWI product has been updated. For details see the Scatterometer cyclic report - cycle 90 -. The Figure 28 (since beginning of HEY dissemination) and Figure 29 (cycle) show for each orbit the average Doppler frequency shift (first 3 plots Fore Mid and Aft antenna), the minimum, maximum and mean yaw (fourth plot), the yaw standard deviation (fifth plot) and the percentage of source packets acquired with a yaw error angle outside the range +/- 2 degrees (sixth plot). On average the yaw evolution is within the specification for the ESACA processor to assure calibrated data. The evolving yaw bias occurred in June 2004 has been reported to the flight segment and corrective actions have been put in place to compensate for.

The result of the monitoring for cycle 138 is an average (per orbit) yaw error angle within the expected nominal range (+/- 2 degrees) for most of the orbit.
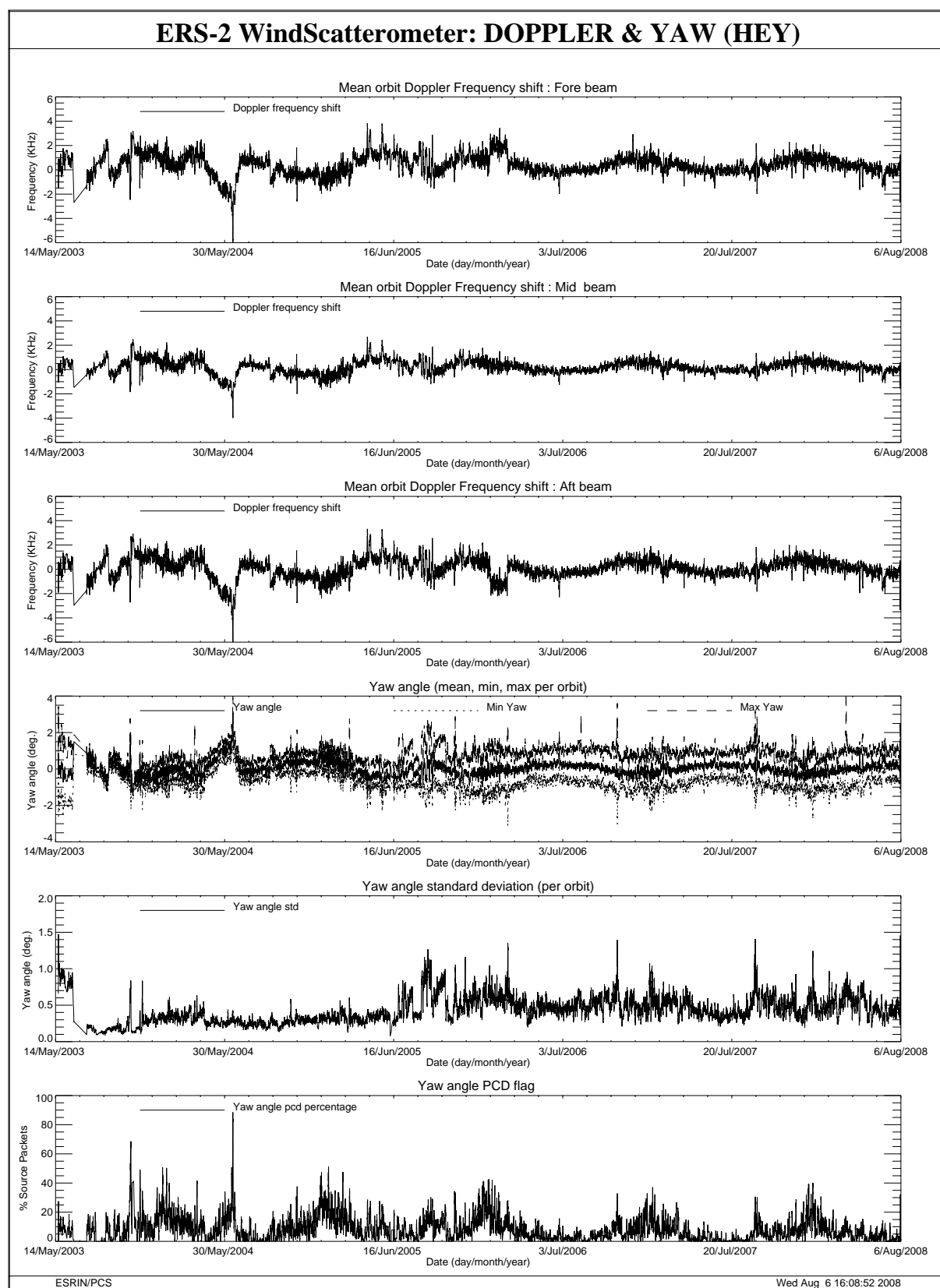
FIGURE 28 Doppler frequency shift and Yaw error angle evolution since August 2003 with a smooth of 14 orbits
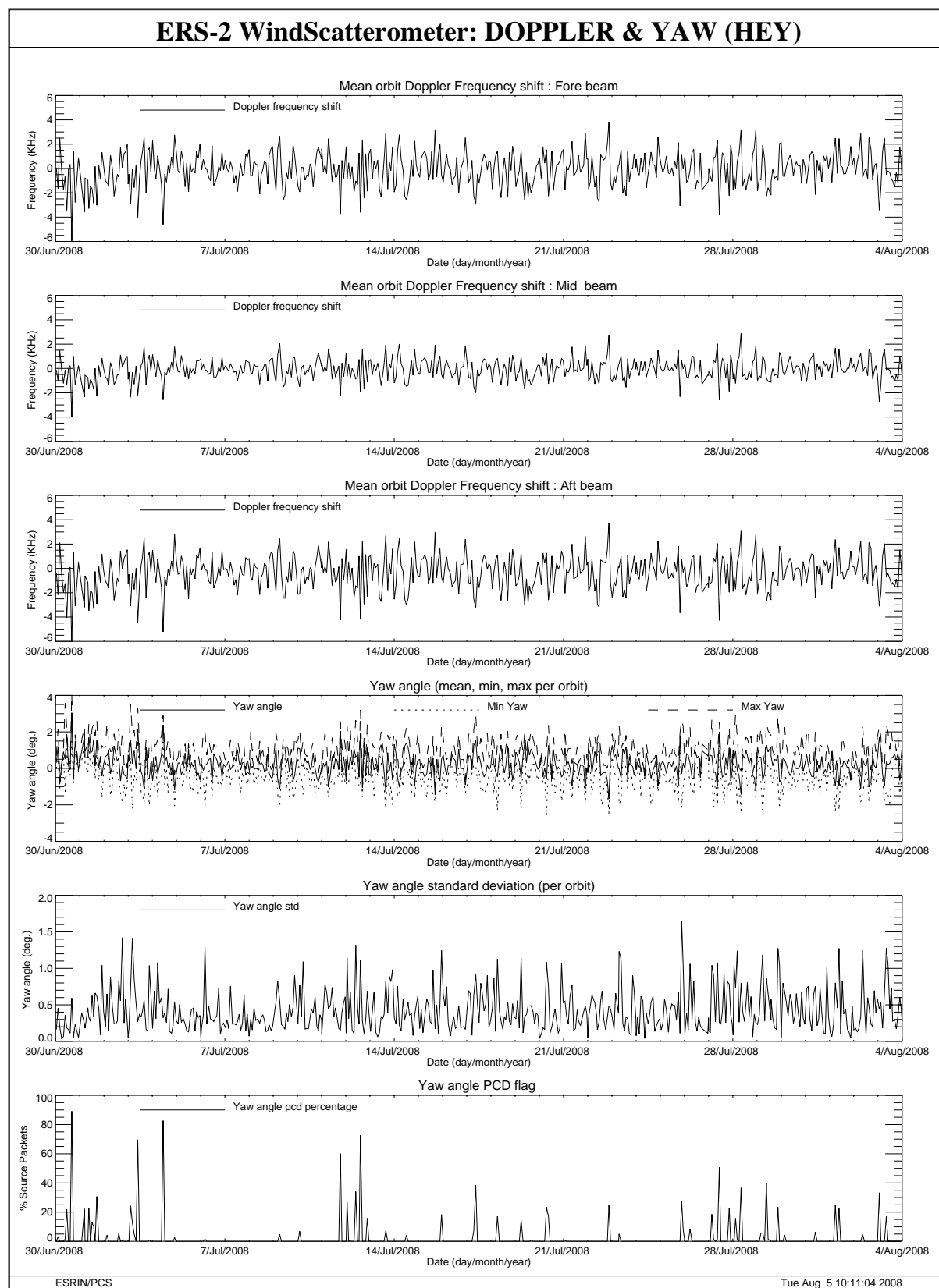
FIGURE 29 Doppler frequency shift and Yaw error angle evolution cycle 138.